



INSTITUTO
UNIVERSITÁRIO
DE LISBOA

**Payload's Sway Angle Measurement for Container in the Crane system
based on Remote Sensing**

YIBIN HU

Master in Telecommunications and Computer Engineering

Supervisors:

Dr. Octavian Adrian Postolache, Associate Professor with Habilitation
ISCTE-Instituto Universitario de Lisboa

Dr. Weimin Xu, Assistant Professor
Shanghai Maritime University

November, 2020



TECNOLOGIAS
E ARQUITETURA

Department of Information Science and Technology

**Payload's Sway Angle Measurement for Container in the Crane system
based on Remote Sensing**

YIBIN HU

Master in Telecommunications and Computer Engineering

Supervisors:

Dr. Octavian Adrian Postolache, Associate Professor with Habilitation
ISCTE-Instituto Univesritario de Lisboa

Dr. Weimin Xu, Assistant Professor
Shanghai Maritime University

November, 2020

Direitos de cópia ou Copyright

©Copyright: Nome Completo do(a) candidato(a).

O Iscte - Instituto Universitário de Lisboa tem o direito, perpétuo e sem limites geográficos, de arquivar e publicitar este trabalho através de exemplares impressos reproduzidos em papel ou de forma digital, ou por qualquer outro meio conhecido ou que venha a ser inventado, de o divulgar através de repositórios científicos e de admitir a sua cópia e distribuição com objetivos educacionais ou de investigação, não comerciais, desde que seja dado crédito ao autor e editor.

Acknowledgments

First, I would like to express my sincere thanks to my advisor, Professor Octavian Postolache and Prof. Weimin Xu, for all the availability and support during the realization of this research.

Special thanks go to Instituto de Telecomunicacoes and Iscte-Instituto Universiario de Lisboa that provide all the equipments and other resoures needed for this dissertation.

My biggest thanks go to my family for unconditional support, especially to my parents, Chenqiu Hu and Julin Chen, and my sister, Liuting Hu.

Special thanks to my long-time friends, Chen Ye and Yuankang Gao, for all the encouragement and for, in some way, helping me through this project.

At the end, a huge thanks to my friends and colleagues who accompanied me on this journey, especially to Mariana Jacob Rodrigues, Barbara Costa, and Joao Monge for the discussions of ideas that really helped me complete this project.

Resumo

A demanda por um ângulo de medição rápido e alto no sistema de guindaste portuário deve ser considerada quando o contêiner for transferido de um local para outro. É significativo construir a ligação de feedback do ângulo da carga útil no sistema de guindaste integrado. O valor da medição precisa do ângulo pode ser usado para otimizar o sistema de controle do guindaste. Neste contexto, será realizada a concepção e implementação da configuração experimental associada a gruas emuladas. Diversas soluções para medição remota de ângulos foram consideradas uma das soluções consideradas sendo representadas por sensores de micro-ondas milimetrados. Desenvolvimentos especiais de algoritmos para calcular o ângulo de oscilação da carga útil ou contêiner foram considerados, assim como o processamento em tempo real usando a plataforma de computação Arduino Uno. Os seguintes objetivos foram alcançados com sucesso.

1. Desenvolvimento de sistema de sensoriamento remoto para medição do ângulo de oscilação da carga útil considerando radares como os dispositivos de detecção;
2. Desenvolvimento de um novo algoritmo de medição de ângulos e processamento de dados em tempo real;
3. Desenvolvimento de um protótipo caracterizado por processamento em tempo real e capacidade de detecção remota considerando medições de curto e longo alcance, como sensor LIDAR ou sensor de radar.

Palavras-Chave: Sistema de Guindaste Suspenso; Medição de Ângulo; Sensoriamento Remoto; Sensor de Radar.

Abstract

The demand for a high quickly measuring angle in the port crane system should be considered when the container has been transferred from one place to another place. It is significant to build the feedback linking of payload's angle in the integrated crane system. The value of accurate measurement of the angle can be used to optimize the crane control system. In this context, the design and implementation of the experimental setup associated with emulated cranes will be carried out. Several solutions for remote angle measurement were considered one of the considered solutions being represented by millimeter microwave radar sensors. Special developments of algorithms to calculate the sway angle of payload or container were considered as so as the real-time processing using Arduino Uno computation platform. The following objectives were successfully reached.

1. Development of remote sensing system for payload's swing angle measurement considering radars such the sensing devices;
2. Development of a novel angle algorithm measurement and real-time processing of data;
3. Development of a prototype characterized by real-time processing and remote detection capabilities considering short-range and long-range measurements, such as lidar sensor or radar sensor.

Keywords: Overhead Crane System; Angle Measurement; Remote Sensing; Radar Sensor.

Contents

Acknowledgments	i
Resumo	ii
Abstract	iii
Contents	iv
Table Index	vi
Figures Index	vii
Glossary of Abbreviations and Acronyms	ix
Chapter 1 – Introduction	1
1.1. Motivation and Overview	1
1.2. Objectives and Research Questions	3
1.3. Research and Planning Method	5
1.4. Structure of the Dissertation	6
Chapter 2 – State of the Art	7
2.1. Existing Projects	7
2.1.1. Radio Detection and Ranging System (RADAR)	7
2.1.2. Light Detection and Ranging System (LiDAR)	10
2.1.3. Angle measurement system	13
2.2. Communications Protocols	16
2.2.1. Universal Asynchronous Receiver/Transmitter communication protocol	16
2.2.2. Inter-integrated circuit (I2C) communication protocol	19
Chapter 3 – System and Method Description	23
3.1. Overview	23
3.2. 1-D Radar Detection Method for Sway Angle	25
3.3. 2-D Radar Detection Method for Sway Angle	28
Chapter 4 – Hardware	31
4.1. Overhead Crane Frame	31
4.2. Overhead Crane Trolley	33
4.3. Payload or Container	35
4.4. SP25 Millimeter-wave Radars	36
4.5. LIDAR Sensor	42
4.6. Microcontroller - Arduino Uno Rev3	45
Chapter 5 – Software	47
5.1. Arduino IDE	47
5.1.1. Introduction of Arduino IDE	47
5.1.2. Basic functions for an application	47
5.2. Matlab Simulink Simscape	52

5.3.	MATLAB.....	53
5.3.1.	Why choose m-file?.....	53
5.3.2.	The analysis process for container data.....	53
Chapter 6 –	Simulation Results and Discussions	56
6.1.	Simscape Multibody Recap	56
6.2.	Simulation System	56
6.2.1.	Overhead crane model structure	57
6.2.2.	Subsystems description	58
6.3.	Simulation Results	60
6.3.1.	The fixed payload	60
6.3.2.	The moving payload	64
Chapter 7 –	Experimental Results and Discussions.....	67
7.1.	Obtain the Data from the SP25 mm-Wave Radar.....	67
7.2.	Testing Results of SP25 mm-Wave Radar	70
Chapter 8 –	Conclusions and Future Work.....	71
8.1.	Conclusions.....	71
8.2.	Future Work.....	73
References.....		75
Annex A.....		80
Annex B.....		81
Annex C.....		87

Table Index

Table 1 – Format of I2C addresses	21
Table 2 – Parameters description 1	26
Table 3 – Parameters description 2	28
Table 4 – Specification of Test overhead crane	32
Table 5 – Specification of payload	35
Table 6 – SP25 Specifications	37
Table 7 – Format of data message	39
Table 8 – Definition of Message-ID	39
Table 9 – Format of data message 0x70C	40
Table 10 – Physical features of Lidar	43
Table 11 – Electrical features of Lidar	43
Table 12 – The description of each pin	44

Figures Index

Figure 1 – JORN radar locations and coverage.....	8
Figure 2 – Surface movement radar.	9
Figure 3 – Detecting all available assets	9
Figure 4 – The radar scan physical properties of the observed surfaces.	10
Figure 5 – The weather radar observations.	10
Figure 6 – The simple principle of LiDAR	11
Figure 7 – The Airborne LiDAR systems	12
Figure 8 – The Leica TerrainMapper-2	12
Figure 9 – The Terrestrial LiDAR systems	13
Figure 10 – The baud rates calculation of UART.	16
Figure 11 – The UART data transfer connection	17
Figure 12 – The definition of Uart data	18
Figure 13 – Transfer conditon for starting or stopping I2C	20
Figure 14 – The start and stop condition associated with SDA and SCL signals	20
Figure 15 – I2C data transfer	21
Figure 16 – The definition of I2C address.....	21
Figure 17 – One model of overhead crane with swaying container	23
Figure 18 – An angle measurement system.....	24
Figure 19 – The basic parts of an overhead crane	25
Figure 20 – 1-D Radar detection system diagram.	26
Figure 21 – 2-D Radar detection system diagram.	28
Figure 22 – The definition of cosine angle for vector	29
Figure 23 –The definition of cosine between two planes.....	30
Figure 24 – Makerbeam Aluminum Alloy Bracket.....	31
Figure 25 – Makerbeam Bracket Corner	32
Figure 26 – Makerbeam M3 6mm Wing Bolt	32
Figure 27 – Overhead crane.....	33
Figure 28 – The detail structure of trolley	33
Figure 29 – The structure of trolley in the lab.....	34
Figure 30 – The wood panel for trolley	34
Figure 31 – The container in the lab test	35
Figure 32 – The SP25 radar sensor.....	37
Figure 33 – The SP25 radar sensor in the lab test	37
Figure 35 – Connection of SP25 radar to serial port	38
Figure 36 – LIDAR-Lite v3.....	42
Figure 37 – I2C connection diagrams of Lidar sensor	44
Figure 38 – Arduino Uno Rec3	45
Figure 39 –The flow chart for whole Lidar to detect distance.	48
Figure 40 –The result of distance for trolley.	49
Figure 41 – The flow chart for configuring lidar's work mode.	49
Figure 42 – The flow chart about the detail of distance reading.	50
Figure 43 – Simscape product family.....	52
Figure 44 – Flow chart for the meassage ID = 0x70C processing.	54
Figure 45 – 3D Animation.....	56
Figure 46 – The physical model of overhead crane system	57
Figure 47 – The structure of overhead crane model.....	58
Figure 48 – The diagram of Lidar sensor	58
Figure 49 – The diagram of radar sensor.....	59

Figure 50 – The diagram of moving payload	59
Figure 51 – The diagram of fixed payload	59
Figure 52 – The dynamic picture of fixed payload	60
Figure 53 – The graph result from fixed payload.....	61
Figure 54 – The evolution of distance and sway angle for the particular case of Distance of trolley, $d=0.6\text{m}$, Length of rope, $l=0.45\text{m}$ (simulation)	62
Figure 55 –The evolution of distance, sway angle for the particular case of Distance of trolley, $d=0.6\text{m}$, Length of rope, $l=0.35\text{m}$ (simulation).....	62
Figure 56 – The evolution of distance and sway angle for the particular case of Distance of trolley, $d=0.6\text{m}$, Length of rope, $l=0.25\text{m}$ (simulation)	63
Figure 57 –The evolution of distance and sway angle for the particular case of Distance of trolley, $d=0.4\text{m}$, Length of rope, $l=0.35\text{m}$ (simulation)	63
Figure 58 – The dynamic picture of moving payload	64
Figure 59 – A given position signal for moving payload.....	65
Figure 60 – The result of angle information for moving payload	65
Figure 61 – Experimental setup.....	67
Figure 62 – Initial configurations for serial port using Matlab	68
Figure 63 – Data processings for radar sensor	68
Figure 64 – Experimental results, for the distance of trolley $d=0.49\text{m}$	70
Figure 65 – The diagram for sensor fusion technologies.	73

Glossary of Abbreviations and Acronyms

GUI – Graphical User Interface

ID – Identification

ADC – Analog Digital Convert

RF – Radio Frequency

AGC – Automatic Gain Control

DC – Direct Current

SPI – Serial Peripheral Interface

HSPI – High Serial Peripheral Interface

UAV – Unmanned Aerial Vehicle

SOC – System on a Chip

IDE – Integrated development environment

OS – Operation System

CCD – Charge Coupled Device

RADAR – Radio Detection and Ranging

mm-Wave – millimetre -Wave

UART – Universal Asynchronous Receiver/Transmitter

TTL – Time To Live

SNR – Signal Noise Ratio

RCS – Radar-Cross Section

LCD – Liquid Crystal Display

I2C – Inter-Integrated Circuit

SPI – Serial Peripheral Interface

CAN – Controller Area Network

USB – Universal Serial Bus

SDA – Synchronous Data Adapter

SCL – Serial Communication Loop

PC – Personal Computer

FMCW -- Frequency Modulated Continuous Wave

MCU – Micro-Controller Units

COM – Cluster Communication

HIL – Hardware-In-the-Loop

CAD – Computer Aided Design

PTC – Positive Temperature Coefficient

Etc.

Chapter 1 – Introduction

1.1. Motivation and Overview

For hundred of years, human populations have been used cranes in order to aid in the process of moving and lifting heavy objects [1]. The invention of the crane has been largely attributed to ancient Greece, where these early devices were typically powered by men or animals.

Overhead cranes are one crane that is commonly used place in industrial environments. Here we take a brief look back at the history of the overhead crane and how it became a staple and indeed essential component of numerous manufacturing industries.

The first overhead cranes, powered by steam, were developed by a German company in the 1830s [2] and entered mass production in Germany in the 1840s. The overhead crane's origins in England lie in the 18th-century industrial revolution. In 1876 a Liverpool engineer by the name of Sampson Moore designed and produced the first overhead electric crane [3], which was used to hoist guns at the Gun Factory of the Royal Arsenal in London. Overhead cranes subsequently came to be used extensively in the steel manufacturing factories driving the industrial revolution.

Since the advent of the industrial revolution, the overhead crane has been employed in a wide variety of different applications and there have been a significant number of new innovations, which have seen the overhead crane undergo significant modernization. Overhead cranes are still widely used in the manufacturing of steel as well as several other key industries [4], such as the refinement of other metals including copper, the automotive industry, and the port of Misburger (Hannover) [5]. Furthermore, modern overhead cranes are also available in smaller scaled-down versions, suitable for use in smaller enterprises and applications to aid in the lifting and moving process.

Overhead cranes are necessary at many job sites. When you've got to lift and move heavy loads, overhead cranes increase floor space, safety, and efficiency. Bridge cranes [6], gantry cranes [7], and other types of overhead cranes are critical to many industries and to the economy. Here are some industries that use overhead cranes to perform their job safely and efficiently. 1) Shipbuilding [8], Ship hulls are massive and irregularly shaped. Moving heavy tools and parts around the inside of a slanted hull can be impossible without an overhead crane. A wide-spanning heavy gantry crane is a must for building ship hulls. 2) Transportation [9], the most visible overhead cranes are the

massive units loading and unloading ships at seaports [10]. The seaport is the gateway of international commerce, and these busy sites have massive products coming and going constantly.

Overhead cranes have recently become a focus of research in modern industrial fields. To increase productivity, the overhead crane transports the payload as fast as possible to its destination.

The overhead cranes of port increasingly play a huge role in modern society, because the international trades are occupying the market all around the world. Therefore, the supplier of overhead cranes should pay more attention to the performance of overhead cranes, so that avoiding the accident. There are two key parts of the research, which including payload's positioning and its anti-swing [11] of the angle when the container was been transferred.

As far as anti-swing control for containers during the transit by overhead crane, the angle of the container should be measured. Therefore, the demand for a high quickly measuring angle in the overhead crane system should be considered, when the container has been transferred from one place to another place in the ports. It is pretty significant to build the feedback of sway angle in the control system linking to the integrated crane system. The value of accurate measurement of the angle can be used to optimize the crane control system.

In this context, the design and implementation of an experimental setup associated with emulated cranes will be carried out considering the possibility to measure the angles in a remote way by using microwave radars. Special developments of algorithms to calculate the angle of the payload will be considered as so as the real-time processing and communication using platforms.

1.2. Objectives and Research Questions

The objective of this research is to develop a container's sway angle detection system capable of retrieving and storing data received from sensors that are attached to an anti-waving control crane used by the controller that is in a real process of operation. This system should allow the crane's operator to visualize the container's working status and overall progress. Based on those results of sway angle, the crane's operator should be able to make new decisions or try new approaches to the controlling sessions in case the progress is moving trolley with over acceleration or less deceleration.

When designed the measurement system for payload's angle, what objectives should be considered as following:

1. Perform a state of the art concerning existing remote sensing solutions referred in the literature, algorithms and real time platforms for appropriate implementation and communication;
2. Develop a prototype with real-time processing and wireless communication capabilities considering short range and long-range communication;
3. Develop a prototype for angle measurement associated with crane operation, with good accuracy and real-time state feedback to the overhead crane control system.
4. Develop a friendly GUI and data storage during the system operation
5. Write and publish an article in a journal or/and conference proceeding with peer - review;
6. Write the MSc thesis.

This project aims to solve some certain questions, such as:

1. Will the remote sensing system for payload's angle measurement considering radars be useful?
2. Can the novel angle measurements algorithm assures higher real-time of the process of angle calculation?
3. Will the remote sensing system and experimental setup including hardware and software components be easy to establish?
4. Will these algorithms for payloads's angle be an accurate measurement?

5. Which simulation and appropriate experimental protocols are good for the system validation?

1.3. Research and Planning Method

The research method used in this project is divided in 7 different steps described below:

1st Step → Identifying the problem - In this phase it is important to understand the lack of technology currently used in angle measurement so we can set objectives to improve overall detection approaches;

2nd Step → Definition of objectives - This step involves the study and the choice of different technologies and materials that can be used and distinguished by radar wave;

3rd Step → System prototype development and construction - Several components of the project are developed at this stage, such as:

- Design and implementation of a miniature overhead crane;
- Design and implementation of an angle detection system based on microwave radar to be attached to an overhead crane;
- Development of a trolley position model based on laser sensor to be attached to a track of it;

4th Step → System prototype implementation - By implementing the components in the previous stage, a project prototype will be created;

5th Step → System prototype simulation – By Matlab Simulink establishing a physical model simulation, such as:

- Development and creation of virtual overhead crane by Simscape Multibody;
- Creation of analyses algorithm for data processing.

6th Step → System prototype tests - Series of tests, adjustments and modifications to the system prototype will be performed in order to obtain a final prototype;

7th Step → Evaluation - The final prototype of the project obtained in the last step must be tested and evaluated.

1.4. Structure of the Dissertation

This dissertation is divided into seven chapters:

Chapter 2 includes a literature review where some sensors can be applied in the sway angle measurement.

Chapter 3 describes this project's measurement system description

Chapter 4 contains all the hardware used in the project, including radar sensors, laser sensors, microcontrollers, and payload devices, motor.

Chapter 5 describes the software used, such as the android studio.

Chapter 6 considers the simulation results and processed data of the sway angle.

Chapter 7 considers the experimental results and processed data of the sway angle.

Chapter 8 mentions the conclusions of the project and future work.

Chapter 2 – State of the Art

This chapter presents the research on sensors used in the detection angle area, more specifically payload's angle. The existing projects researched and presented below provide new measurement ways of container's angle to ensure that the anti-waving controller has real-time and accurate feedback of the swing angle.

2.1. Existing Projects

2.1.1. Radio Detection and Ranging System (RADAR)

RADAR stands for Radio Detection and Ranging System [39]. It is basically an electromagnetic system used to detect the location and distance of an object from the point where the RADAR is placed. It works by radiating energy into space and monitoring the echo or reflected signal from the objects. A basic RADAR system consists of 6 major parts [40], as follows:

- **A Transmitter:** The signal is first generated using a waveform generator and then amplified in the power amplifier.
- **Waveguides:** The waveguides are transmission lines for transmission of the RADAR signals.
- **Antenna:** The antenna used can be a parabolic reflector, planar arrays or electronically steered phased arrays.
- **Duplexer:** It can be a gaseous device that would produce a short circuit at the input to the receiver when transmitter is working.
- **Receiver:** It can be super heterodyne receiver or any other receiver which consists of a processor to process the signal and detect it.
- **Threshold Decision:** The output of the receiver is compared with a threshold to detect the presence of any object.

There are two types of radar systems [39]: one is Pulse RADAR, which sends high power and frequency pulses towards the target object. The range will depend on pulse repetition frequency; another one is Continuous Wave RADAR, which doesn't measure the range of the target but rather the rate of change of range by measuring the Doppler shift of the return signal.

There are many fields in a society where radar has been used, such as Military Applications, Air Traffic Control, Ground Traffic Control, and Remote Sensing[40].

1) Military Applications: In Air defence as it is used for target detection.

Radar was initially discovered and developed for use by the military to advance military activities around the world. Military radars are used to all mobile, fixed, and transportable 2-D and 3-D systems used in the air defence mission. At present,

Jindalee Operational Radar Network (JORN) (shown as Figure 1) is the world's largest air defence radar. JORN is a network of three remote OTHR radars located in the Northern Territory, Queensland and Western Australia. [41]. The Australian Defence Force (ADF) currently operates three OTHR systems as part of the Jindalee Operational Radar Network (JORN). These radars are dispersed across Australia — at Longreach in Queensland, Laverton in Western Australia and Alice Springs in the Northern Territory — to provide surveillance coverage of Australia's northern approaches[42].



Figure 1 – JORN radar locations and coverage.

2) Air Traffic Control: It is to guide the aircraft to land in bad weather using precision approach radar.

Air Traffic Control Radar (ATC-Radar) [43] is the umbrella term for all radar devices used to secure and monitor civil and military air traffic in Air Traffic Management (ATM). There are some common applications of ATC-Radar, which include en-route radar systems, Air Surveillance Radar (ASR) systems, Precision Approach Radar (PAR) systems, surface movement radars (Figure 2), and special weather radars. They are usually fixed radar systems that have a high degree of specialization.



Figure 2 – Surface movement radar.

- 3) *Ground Traffic Control: RADAR can also be used by traffic police to determine speed of the vehicle.*

Ground Traffic Control (GTC) [44] is a next-generation software and hardware solution for all vehicle traffic at a test track including ADAS platforms, human and robot-controlled vehicles along with fixed proving ground infrastructure like traffic lights and barriers. GTC has some major fundamental functions, includes collision detection and prevention, advanced monitoring of vehicle, and detecting all available assets on the proving ground or road, as shown in Figure 3.



Figure 3 – Detecting all available assets

- 4) *Remote Sensing: RADAR can be used for monitoring weather, planetary positions and observing sea ice.*

A satellite-based synthetic aperture radar (Synthetic Aperture Radar, SAR) (shown as Figure 4) [45] scans the earth's surface by means of microwave radiation. The SAR

antenna transmits microwave pulses and receives the backscattered echo from the surface. Based on this echo high-resolution image data and data products can be produced.

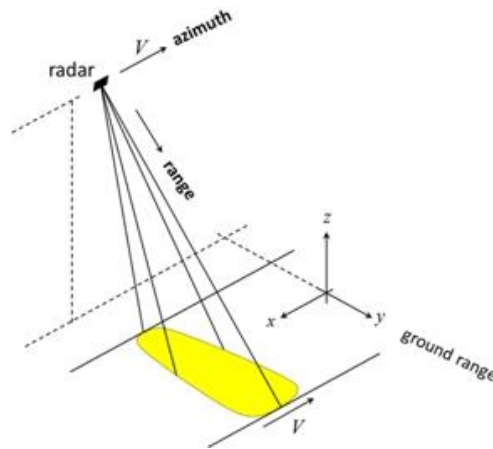


Figure 4 – The radar scan physical properties of the observed surfaces.

The SAR technology has several special features in comparison to other imaging remote sensing methods. On the one hand, it is possible to observe the Earth's surface even on cloudy days and at night. On the other hand, physical variables such as the backscattering coefficient or path length differences in the viewing direction of the SAR antenna can be derived. Radar uses relative long wavelengths which allows these systems to "see" through clouds, smoke, and some vegetation. Radar can be used for observing weather[46], such as Weather Radar Observations in Figure 5.



Figure 5 – The weather radar observations.

2.1.2. Light Detection and Ranging System (LiDAR)

LiDAR, or light detection and ranging, is a popular remote sensing method used for measuring the exact distance of an object on the earth's surface [47]. According to the American Geoscience Institute, LiDAR uses a pulsed laser to calculate an object's

variable distances from the earth surface. There are three primary components of a LiDAR instrument—the scanner, laser and GPS receiver. Most social companies and private organizations use airplanes, drones and helicopters for acquiring LiDAR data. As we can know, there are two types of Lidar system based on its functionality, for instance airborne LiDAR and terrestrial LiDAR. Airborne LiDAR systems are installed on a helicopter or drone for collecting data, while terrestrial LiDAR systems are installed on moving vehicles or tripods on the earth surface for collecting accurate data points.

LiDAR follows a simple principle — throw laser light at an object on the target (object) surface and calculate the time it takes to return to the LiDAR source as shown in Figure 6. The formula that analysts use to arrive at the precise distance of the target (object) is as follows:

$$\text{The distance of the object} = (\text{Speed of Light} \times \text{Time of Flight}) / 2$$

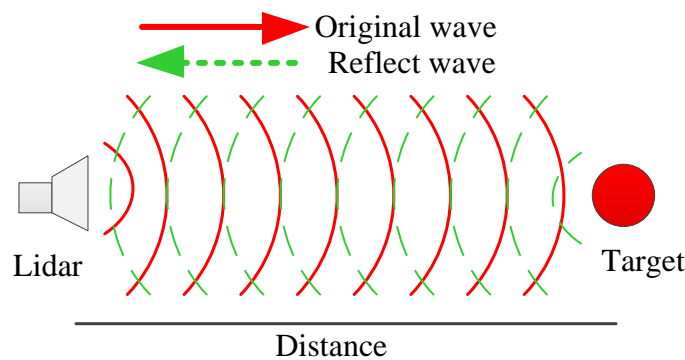


Figure 6 – The simple principle of LiDAR

1) Airborne LiDAR

The LiDAR technology can implement in the Airborne LiDAR systems, as a simple model in Figure 7. One of searching product is Airborne Laser Scanning, which can be mounted on aerial vehicles such as aircraft and helicopters. LiDAR technology enables the automated acquisition of 3-dimensional data at a high rate. Weather and visibility hardly affect measurements, making these systems ideal for any surveying, inspection or mapping.

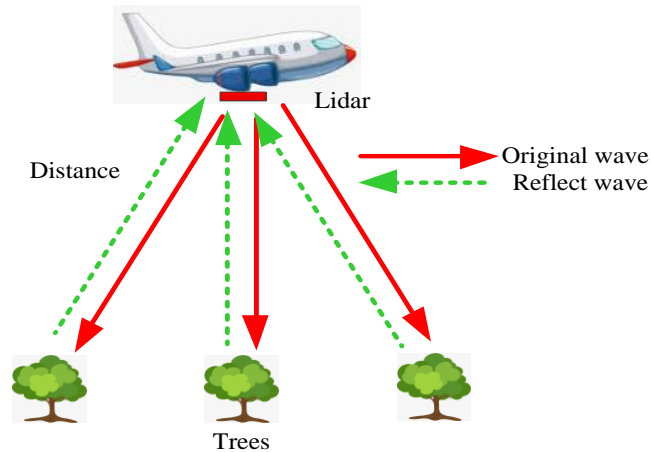


Figure 7 – The Airborne LiDAR systems

As shown in Figure 8, the Leica TerrainMapper-2[48] is the latest linear-mode LiDAR airborne sensor providing the highest performance for regional mapping projects. It has some important features: 1) Gateless MpiA delivers outstanding accuracy, 2) unmatched point density and even 3) point distribution. It can work at high altitude applications.



Figure 8 – The Leica TerrainMapper-2

2) Terrestrial LiDAR

Terrestrial Laser Scanning (TLS) offers the opportunity to collect high-precision and high-accuracy data over large spatial extents, at temporal frequencies commensurate with individual flood events [49]. TLS instruments are commonly broken into three categories based on the distance the laser light can travel to record a point in a field-of-view: short-, medium- and long-range scanners, such as a model in Figure 9. TLS devices optimised for a long-range (several hundreds of metres to kilometres) have been applied to measuring spatially larger areas. For short-range scanners, the interval between adjacent measurement points can be up to 1 mm, although such densities are not practical for all

but the smallest areas [49]. SAM utilizes terrestrial laser scanning tools to perform High Definition Surveying, also known as HDS. These are the most advanced terrestrial laser scanning systems on the market, allowing us to unobtrusively deliver data of high quality and accurate detail in a significantly shorter project cycle [50].

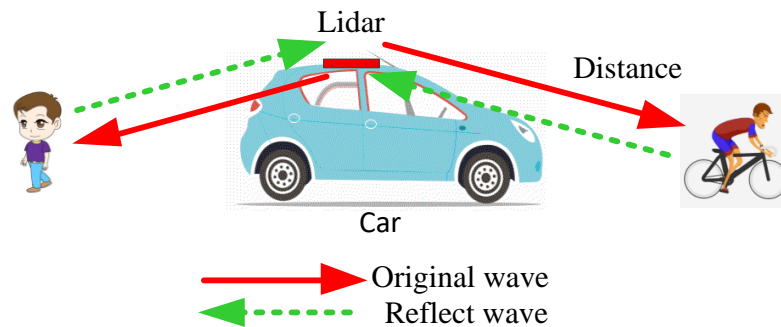


Figure 9 – The Terrestrial LiDAR systems

2.1.3. Angle measurement system

The angle measurement system is a concept with great development, with the potential to alter the way we see the technological world.

Over the past decades, overhead cranes [12] have been widely used in some transport areas for moving heavy goods, such as ports, industries, and railway transportations. During the work of overhead cranes, some exterior factors, for example, winds, will affect it and cause the payloads to sway, which will reduce the performance of overhead crane system for transport of goods. So, it is necessary to overcome those problems that anti-swing control of the system of overhead crane, positioning of trolleys and payloads and measuring sway angle of payloads. However, the real-time accurate measurement for payload's position and angle is an important precondition for anti-swing control. Therefore, considerable researches have been done for the problem of detecting payload's angle in overhead crane systems, such as using CCD camera, encoder, and laser.

A sway angle measurement is an important task to provide accurate positioning of payloads. In order to gather the value of sway angle for the payload in the crane system, many efforts have been devoted and many interesting methods have been designed. There are two common approaches to measure the sway angle: one is based on sensors and the second one is a sensors-less method. The sensors method can use contact sensors—Encoder, Inclinator, and non-contact sensors—CCD image sensors, Laser tracker, Radar sensors.

A few methods have been proposed in the literature for detecting the sway angle during the movement of trolley or at unmoved points. Thus, in [13], Shimpei et. Al proposes a method to estimate the sway angle of the payload without a sensor, which uses a reaction force observer. It can estimate the power of the motor to suspend the payload with a rope by using the force of the motor [15]. Then, the sway angle can be estimated. The Sano et. al. [14] estimated the sway angle of the payload using the motion equation of the crane system and time compensation observer [15].

To obtain and reach the value of sway angle in an overhead crane system, some sensors are implementing to the spreader, which was connected to the payload. These sensors will be going to move or sway when the motion state of payload has been changed. In [16], an inclinometer is investigated as a sway sensor together with a state observer as a part of a mathematical model. This state observer is a kind of system in control theory, which can estimate the internal state of a real system based on its input and output given the actual system architecture. This observer is used to estimate variables, such as the angular velocity and the trolley velocity in crane system. The measurement of the inclination angle of the spreader and the conversion of the measured value into a sway angle is a base of the method that is presented in [17].

The reliability of the system is low; thus, the inclinometer can be destroyed easily because it was connected to the spreader when the spreader crashes to other mechanical parts. Thus, they consider non-contact sensors, such as CDD image sensors. In [18], Osumi proposed a method by using two CCD cameras. The two CCD cameras were set towards wire on a horizontal plane. The sway angle can be obtained by calculating the two-wire images, which represent the wire of the payload and a vertical line. To achieve the maximum CCD camera performance, [19] design an algorithm to reduce the process of the image, improving the effective.

Because the vision system has many drawbacks such as difficult maintenance, easily affected by weather, and so on, control schemes without the vision system are being investigated nowadays [20]. However, the radar sensor cannot be affected by weather, it is a good choice to measure the sway angle. Thus, the aim is to reduce the cost of the entire system and its simplification. So, the idea of using one mm-Wave radar was born.

The radar (Radio Detection and Ranging) is an electromagnetic system which is used for detection and localization of the conductive objects (targets). The millimeter-Wave (mm-Wave) frequency band is promising for various applications, such as wireless

sensing, imaging, and communications. Its unique characteristics, such as penetration through fog/rain/cloud, all-weather and all-day, can enable a variety of applications, for example, meteorological forecast, resource exploration and environmental monitoring.

2.2. Communications Protocols

This section describes the various communication protocols used in this project. Some I/Os may be hidden on the symbol under the conditions listed in the description. Some features or characters of the communication protocols will be displayed in this section.

2.2.1. Universal Asynchronous Receiver/Transmitter communication protocol

A Universal Asynchronous Receiver/Transmitter (UART) is the microchip with programming that controls a computer's interface to its attached serial devices, such as a single-chip microcomputer and LCD drivers. Specifically, it provides the computer with the RS-232C Data Terminal Equipment (DTE) interface or USB-TTL (Time to live) so that it can "talk" to and exchange data with modems and other serial devices.

There are some fundamental features of Uart as shown as follows:

- Baud rates from 110 to 921600 bps or arbitrary up to 4 Mbps
- Full Duplex, Half Duplex, TX only, and RX only optimized hardware
- RX and TX Buffer Size (bytes)= 4 to 65535
- Detection of Framing, Parity, and Overrun errors

To assist with the processing of the UART receive and transmit data, independent size configurable buffers are provided. The independent circular receives and transit buffers in SRAM and hardware FIFOs help to ensure that data will not be missed. This allows the CPU to spend more time on critical real-time tasks rather than servicing the UART.

Baud rates: The approximate rate (in bits per second, or bps) at which data can be transferred. A more precise definition is the frequency (in bps) corresponding to the time (in seconds) required to transmit one bit of digital data. For example, with a 9600-baud system, one bit requires $1 / (9600 \text{ bps}) \approx 104.2 \mu\text{s}$, as shown in Figure 10. The system cannot transfer 9600 bits of meaningful data per second because additional time is needed for the overhead bits and perhaps for delays between one-byte transmissions.

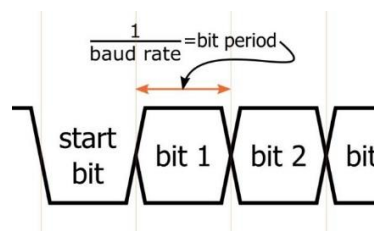


Figure 10 – The baud rates calculation of UART.

Communication Mode: This parameter defines the functional Components.

In UART communication, two UARTs communicate directly with each other, as shown in Figure 11. The transmitting UART converts parallel data from a controlling device like a CPU into serial form, transmits it in serial to the receiving UART, which then converts the serial data back into parallel data for the receiving device. Only two wires are needed to transmit data between two UARTs. Data flows from the Tx pin of the transmitting UART to the Rx pin of the receiving UART. This can be setup to be a bidirectional Full UART (TX + RX) (default), Half Duplex UART (uses half the resources), RS232 Receiver (RX Only) or Transmitter (TX Only).

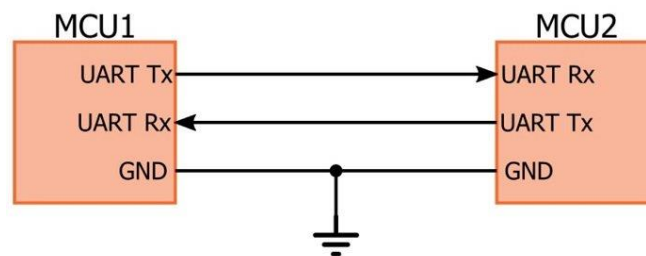


Figure 11 – The UART data transfer connection

RX and TX Buffer Size (bytes): RX Buffer Size (bytes) defines how many bytes of RAM to allocate for an RX buffer. Data is moved from the receive registers into this buffer. TX Buffer Size (bytes) defines how many bytes of RAM to allocate for the TX buffer. Data is written into this buffer. The TX interrupt is not available in Half Duplex mode; therefore, the TX Buffer Size is limited to four bytes when Half Duplex mode is selected.

Start bit: This parameter defines the first bit of a one-byte UART transmission, as shown in Figure. It indicates that the data line is leaving its idle state. The idle state is typically logic high, so the start bit is logic low. The start bit is an overhead bit; this means that it facilitates communication between receiver and transmitter but does not transfer meaningful data.

Stop bit: This parameter defines the last bit of a one-byte UART transmission, as shown in Figure 12. Its logic level is the same as the signal's idle state, i.e., logic high. This is another overhead bit.

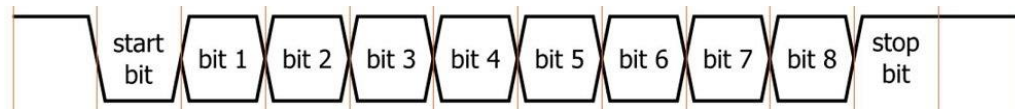


Figure 12 – The definition of Uart data

Parity bit: This parameter defines an error-detection bit added to the end of the byte.

There are two types of parity bit: 1) “odd parity” means that the parity bit will be logic high if the data byte contains an even number of logic-high bits, and 2) “even parity” means that the parity bit will be logic high if the data byte contains an odd number of logic-high bits.

How the uart works?

There are some steps of uart transmission:

Step1: The transmitting UART receives data in parallel from the data bus;

Step2: The transmitting UART adds the start bit, parity bit, and the stop bit(s) to the data frame;

Step3: The entire packet is sent serially from the transmitting UART to the receiving UART. The receiving UART samples the data line at the pre-configured baud rate;

Step4: The receiving UART discards the start bit, parity bit, and stop bit from the data frame;

Step5: The receiving UART converts the serial data back into parallel and transfers it to the data bus on the receiving end.

2.2.2. Inter-integrated circuit (I2C) communication protocol

A typical embedded system consists of one or more microcontrollers and peripheral devices like memories, converters, I/O expanders, LCD drivers, sensors, matrix switches, etc. The complexity and the cost of connecting all those devices together must be kept to a minimum. The system must be designed in such a way that slower devices can communicate with the system without slowing down faster ones [25].

Inter-Integrated Circuit abbreviated as I2C is a serial bus short distance protocol developed by Philips Semiconductor about two decades ago to enhance communication between the core on the board and various other ICs involved around the core [26]. The general concept of serial bus communication is shown in Figure 12. The most popular serial bus communication protocols available today in the market are, SPI, UART, I2C, CAN, USB, IEE1394, and so on. However, Philips originally developed I2C for communication between devices inside of a TV set.

The I2C bus uses two wires: serial data (SDA) and serial clock (SCL). All I2C master and slave devices relate to only those two wires. Each device can be a transmitter, a receiver or both. I2C terminology:

- Transmitter – This is the device that transmits data to the bus
- Receiver – This is the device that receives data from the bus
- Master— This is the device that generates clock, starts communication, sends I2C commands and stops communication
- Slave— This is the device that listens to the bus and is addressed by the master

Serial Data Transfer

For each clock pulse one bit of data is transferred, as shown in Figure 13. The SDA signal can only change when the SCL signal is low – when the clock is high the data should be stable.

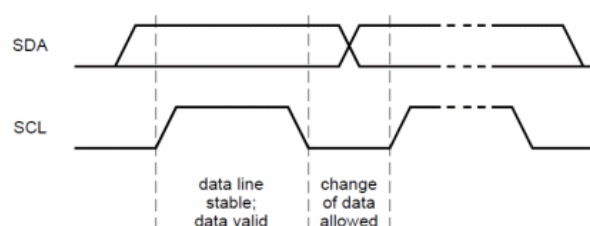


Figure 13 – Transfer condition for starting or stopping I2C

Start and Stop Condition

Every I2C command initiated by the main device begin with a START condition and finish by a STOP condition, as shown in Figure 14. There are two important lines called Synchronous Data Adapter (SDA) and Serial Communication Loop (SCL). The START condition and STOP condition consist of both of SDA and SCL. When SCL are high, the high to low transition of SDA is treated as START and a low to high transition as STOP.

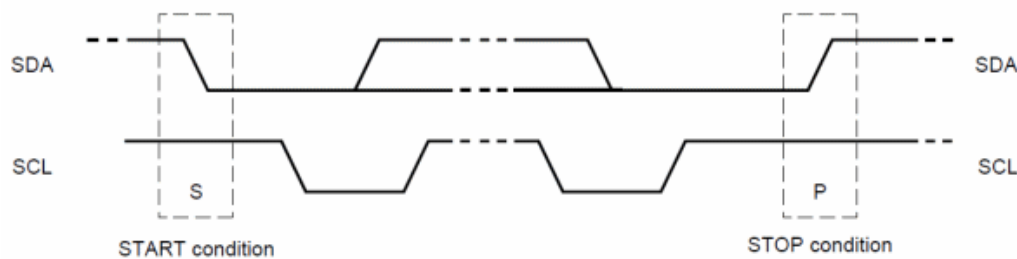


Figure 14 – The start and stop condition associated with SDA and SCL signals

After the Start condition the bus is considered as busy and can be used by another master only after a Stop condition is detected. After the Start condition the master can generate a repeated Start. This is equivalent to a normal Start and is usually followed by the slave I2C address.

Micro-controllers that have dedicated I2C hardware can easily detect bus changes and behave also as I2C slave devices. However, if the I2C communication is implemented in software, the bus signals must be sampled at least two times per clock cycle in order to detect necessary changes.

I2C Data Transfer

Data on the I2C bus is transferred in 8-bit packets (bytes), as shown in Figure 15. There is no limitation on the number of bytes; however, each byte must be followed by an Acknowledge bit. This bit signals whether the device is ready to proceed with the next byte. For all data bits including the Acknowledge bit, the master must generate clock pulses. If the slave device does not acknowledge transfer this means that there is no more data, or the device is not ready for the transfer yet. The master device must either generate Stop or Repeated Start condition.

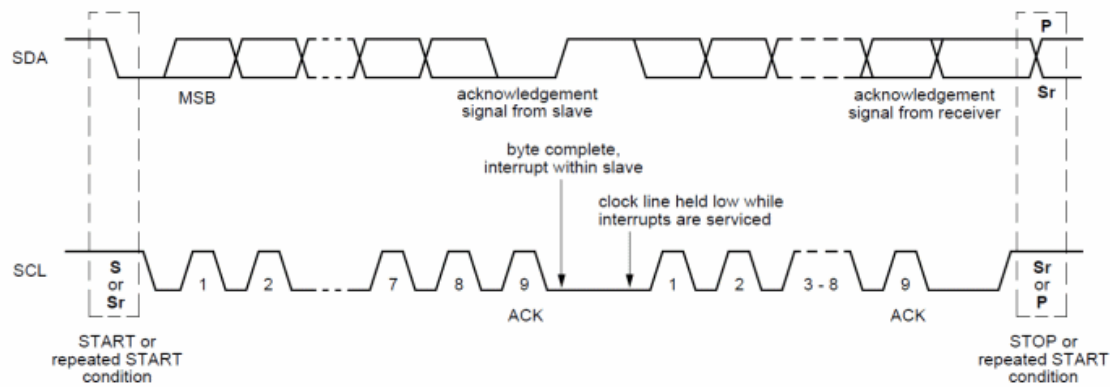


Figure 15 – I2C data transfer

7-bit I2C Addressing

A slave address may contain a fixed and a programmable part. Some slave devices have few bits of the I2C address dependent on the level of address pins, as shown in Figure 16. This way it is possible to have on the same I2C bus more than one I2C device with the same fixed part of I2C address.

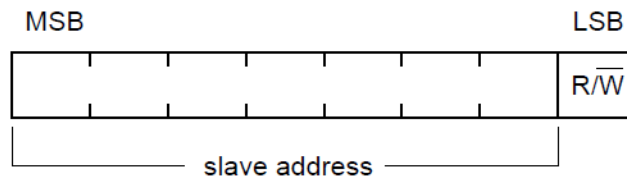


Figure 16 – The definition of I2C address

The allocation of I2C addresses is administered by the I2C bus committee which takes care for the allocations. Two groups of 8 I2C addresses are reserved for future uses and one address is used for 10-bit I2C addressing in Table 1.

Table 1 – Format of I2C addresses

Slave Address	R/W Bit	Description
0000 000	0	General call address
0000 000	1	START byte
0000 001	X	CBUS address
0000 010	X	Reserved for different bus format
0000 011	X	Reserved for future purposes
0000 1XX	X	Hs-mode master code

1111 1XX	X	Reserved for future purposes
1111 0XX	X	10-bit slave addressing

The general call address is used to address all devices on the slave bus. If any slave device doesn't need to respond to such call or general call is not supported by the slave device, the call must be ignored. If the device supports general call and wants to receive the data, it must acknowledge the address and read the data as a slave receiver.

Chapter 3 – System and Method Description

This section describes the angle measurement system and angle calculation method used in this project.

3.1. Overview

As shown in Figure 17, it displays one model of overhead crane, which hold a heavy container. In this situation, the payload is swaying, and the sway angle should be measured. Therefore, for this moment, the radar sensor will be installed in the overhead crane system. This overhead crane system consists of a container, radar sensor, trolley, lidar sensor, Arduino Uno. The lidar sensor is used to measure the distance between the trolley and the Lidar sensor. The radar sensor is used to measure the distance between the container and the radar sensor. Due to the lidar sensor don't have the ability to calculate, the Arduino Uno is used to process the lidar data.

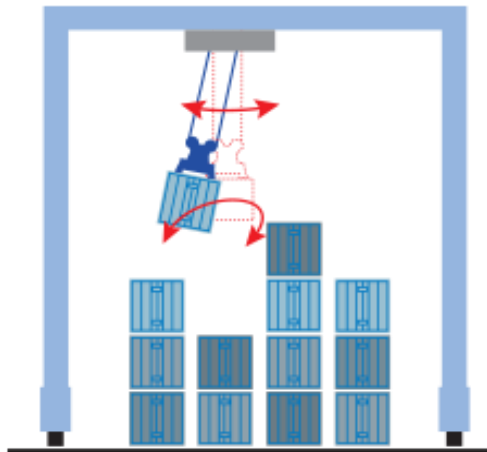


Figure 17 – One model of overhead crane with swaying container

The angle measurement purpose is to be able to measure container's sway angle in the overhead crane that system is affected with trolley activity limitations and clouds or storms, allowing for the crane operators to have access to the angle data obtained from the radar sensor, and, with that data, ensure that the operators or automatic controller are getting the accuracy angle's value. Figure 18 shows the entire system architecture. There are three parts, including distance measurement, position measurement, and data processing. The main function of distance measurement is scanning the distance of container, transferring the data to PC by Uart. The function of position measurement is obtaining the position of the trolley, transferring the original data to Arduino Uno by I2C

and then sending to the PC. The last part is analysing and verifying the result of the method.

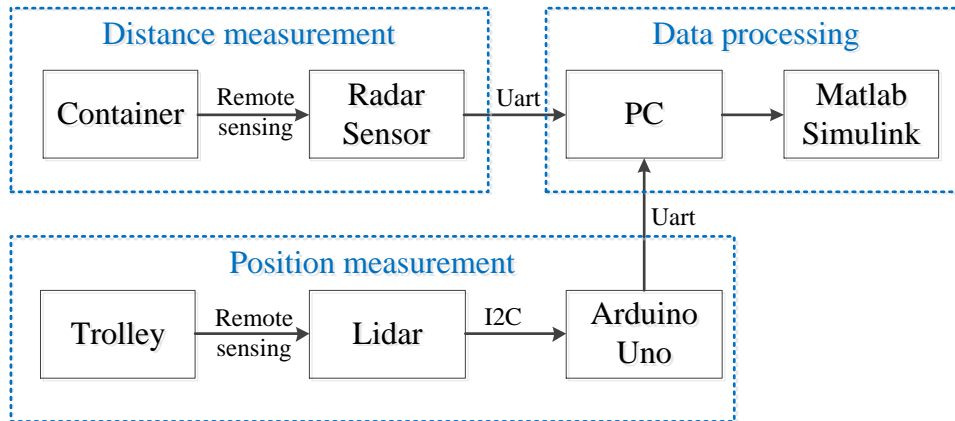


Figure 18 – An angle measurement system

Instead of using a traditional detect device, the overhead system should use a remote sensor so that the operator or controller can monitor trolley's and container's movement. Several contact-less sensors are connected to an Arduino which will then start sending data using UART to the PC device, or directly sent to the PC. Finally, the data will be processed in the Matlab Simulink, which can provide the result of angle information.

This angle measurement system includes two major remote sensors: Radar sensor and Lidar sensor. Each of them plays a different role in this system, providing meaningful information to the processors. The function of data processing is to calculate the actual value of payload's sway angle. It has many causes, which depends on the number of radars.

3.2. 1-D Radar Detection Method for Sway Angle

1-D Overhead crane system and radar system has been shown as Figure 19. This physical system consists of crane supports, rail, trolley, sensor, and the Radar target (payloads, or containers). The transported goods are suspended at the bottom of the trolley by a hook. The radar sensor is mounted on the vertical support of the crane. When the trolley accelerates or decelerates along the crane rail, the payload will swing due to inertia.

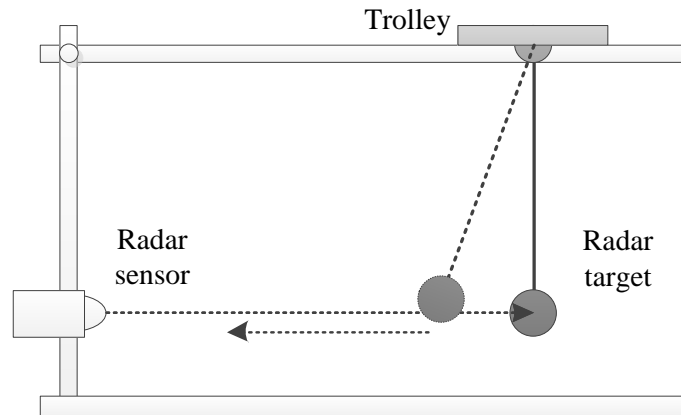


Figure 19 – The basic parts of an overhead crane

The principle of detection will be discussed, as illustrated in Figure 20. As shown in the figure, the vertical support and the trolley tracks are set to the positive directions of the X-axis and the Y-axis, respectively, and the coordinate origin is defined at their intersection. The distance from the trolley to the origin is set as $O(0,0)$; the distance from the radar to the origin is h , assuming that the length of the sling of the load is l . When the car moves and drives the load to swing, the radar can detect the distances from the radar to the car (r_1) and the radar to the payload (r_2). In Table 2, it includes some of the parameters that are considered in description 1.

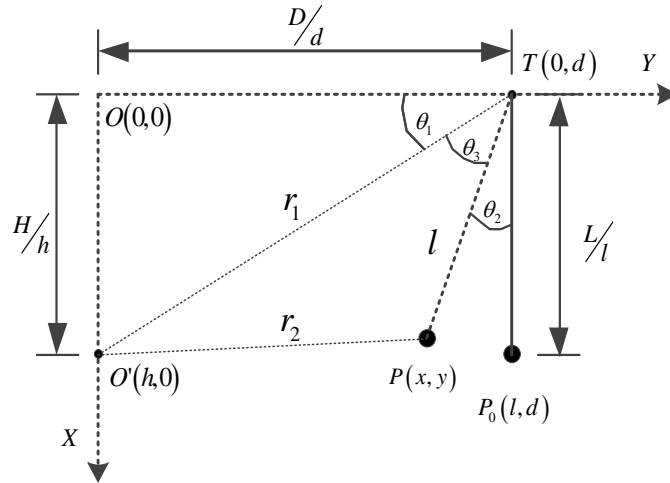


Figure 20 – 1-D Radar detection system diagram.

Table 2 – Parameters description 1

Name	Description
D	Distance measured between the center of the trolley and the origin of the coordinates.
H	Distance measured between the center of the trolley and the origin of the coordinates.
L	Length of the hanging rope.
r_1	Distance measured between the car and the radar.
r_2	Distance measured between the load and the radar.
θ_1	angle between the origin of the coordinates and radar
θ_2	Sway angle of target (load).
θ_3	Angle between the trolley and the radar

Using of the Cosines theory (1) and Tangent rule (2), the value of the θ_1 , θ_2 , angle can be extracted according to them.

$$\cos \theta_3 = \frac{r_1^2 + l^2 - r_2^2}{2r_1l} \quad (1)$$

$$\tan \theta_1 = \frac{h}{d} \quad (2)$$

Due to the relationship of right angle (3):

$$\theta_1 + \theta_2 + \theta_3 = \frac{\pi}{2} \quad (3)$$

Therefore, the sway angle is obtained as formula (4):

$$\theta_2 = \frac{\pi}{2} - \arctan\left(\frac{h}{d}\right) - \arccos\left(\frac{r_1^2 + l^2 - r_2^2}{2r_1l}\right) \quad (4)$$

3.3. 2-D Radar Detection Method for Sway Angle

The principle of measuring two sway angles is shown in Figure 21. The sensor coordinate system is defined as the figure. The axes of the sensor coordinate are set on a horizontal plane near the upper of one of the cranes supports, and the axis is straight down along the support frame from the equilibrium point. Two radar sensors are placed on the middle of the other two crane supports. And Table 3 shows some paraments description 2.

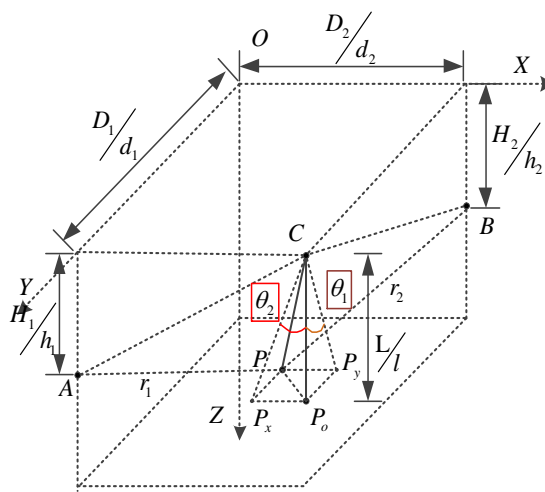


Figure 21 – 2-D Radar detection system diagram.

Table 3 – Paraments description 2

Name	Description
d_1, d_2	Distance measured from trolley to plane ΣXoZ , ΣYoZ
h_1, h_2	Distance measured from the center of radar to plane ΣXoY
l	Length of the hanging rope.
r_1, r_2	Distance measured between the center of radar and the target.
$\theta_1 \theta_2$	Sway angle of target with the vertical line.

According to the definition of coordinate system, the value of each coordinate is obtained as following: $A(0, d_1, h_1)$, $B(d_2, 0, h_2)$, $C(d_2, d_1, 0)$, and $\overline{CP} = (x, y, z)$

Due to $|\overline{AP}| = r_1$ and $|\overline{BP}| = r_2$

The mathematical triangle relationship is defined as follows (5) :

$$\begin{cases} r_1^2 = (x + d_2)^2 + (y)^2 + (z - h_1)^2 \\ r_2^2 = (x)^2 + (y + d_1)^2 + (z - h_2)^2 \end{cases} \quad (5)$$

By expanding equations (5), we obtain

$$\begin{cases} r_1^2 = x^2 + y^2 + z^2 + 2xd_2 - 2zh_1 + d_2^2 + h_1^2 \\ r_2^2 = x^2 + y^2 + z^2 + 2yd_1 - 2zh_2 + d_1^2 + h_2^2 \end{cases} \quad (6)$$

According to the definition of cosine angle, as shown in Figure 22, there are:

$$\begin{cases} \cos \theta_x = \frac{x}{l} \\ \cos \theta_y = \frac{y}{l} \\ \cos \theta_z = \frac{z}{l} \end{cases} \quad (7)$$

From the vector $\overline{CP} = (x, y, z)$, we obtain

$$l^2 = x^2 + y^2 + z^2 \quad (8)$$

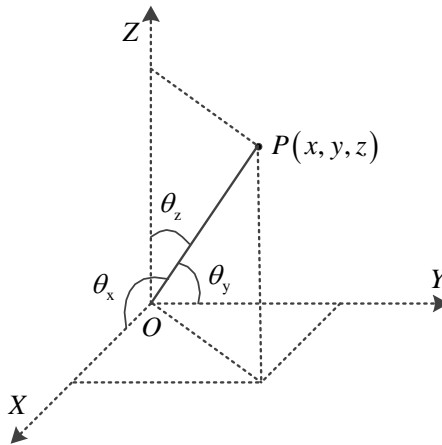


Figure 22 – The definition of cosine angle for vector

By substituting (7), (8) into (6), we obtain

$$\begin{cases} r_1^2 = l^2 + 2 \cos \theta_x l d_2 - 2 \cos \theta_z l h_1 + d_2^2 + h_1^2 \\ r_2^2 = l^2 + 2 \cos \theta_y l d_1 - 2 \cos \theta_z l h_2 + d_1^2 + h_2^2 \end{cases} \quad (9)$$

By solving the equation, we obtain the value θ_x , θ_y , θ_z .

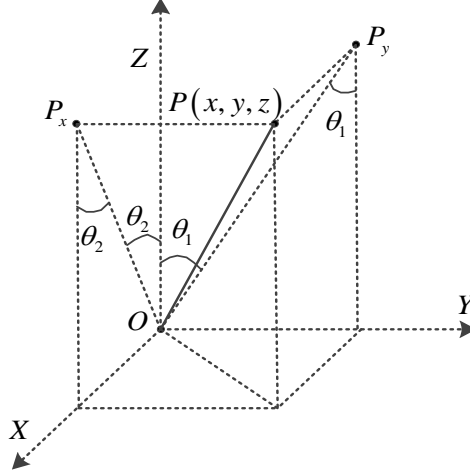


Figure 23 –The definition of cosine between two planes.

According to the definition of cosine Figure 23, the sway angle can be described by the following formula:

$$\begin{cases} \cos \theta_1 = \frac{z}{\sqrt{y^2 + z^2}} \\ \cos \theta_2 = \frac{z}{\sqrt{x^2 + z^2}} \end{cases} \quad (10)$$

By substituting (7) into (10), we obtain (11)

$$\begin{cases} \cos^2 \theta_1 = \frac{\cos^2 \theta_z}{\cos^2 \theta_y + \cos^2 \theta_z} \\ \cos^2 \theta_2 = \frac{\cos^2 \theta_z}{\cos^2 \theta_x + \cos^2 \theta_z} \end{cases} \quad (11)$$

By solving the equation, we obtain the value of sway angle θ_1 , θ_2 .

Chapter 4 – Hardware

After much consideration and research, it was decided that several important hardware components were needed to develop this project, such as:

- Overhead Crane frame as an experimental platform can provide spaces for installing some sensors;
- Trolley that install in the top of crane frame and it can suspend a rope and hook to catch the container;
- Payload or container is a detected target;
- SP25 Millimeter-wave Radars that indicates the distance from payload and radar, it was installed in one side of the crane;
- Lidar sensor capable of positioning the trolley;
- An Arduino Uno capable of processing only Lidar sensor's data.

4.1. Overhead Crane Frame

In order to emulate a real condition of overhead crane for reaching to the reliable result and verifying the accuracy of the proposed method, an overhead crane has been designed for this project in the laboratory. According to the structure of port crane, this experimental crane is composed of the following metal parts -- Makerbeam Clear Anodised – Threaded, Makerbeam Bracket Corner, Makerbeam M3 6mm Wing Bolt, respectively in Figure 24, 25, 26.



Figure 24 – Makerbeam Aluminum Alloy Bracket

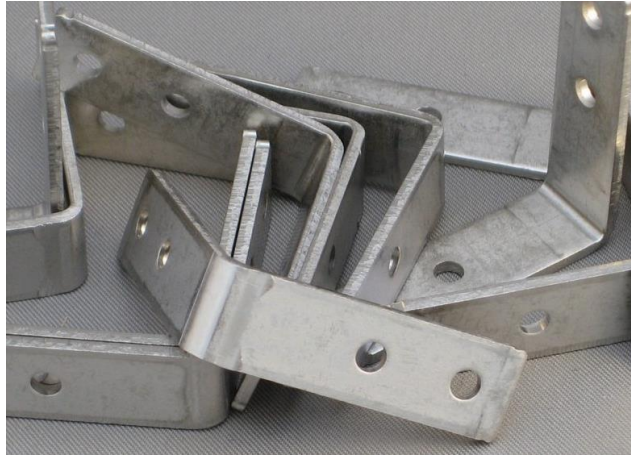


Figure 25 – Makerbeam Bracket Corner



Figure 26 – Makerbeam M3 6mm Wing Bolt

Finally, this experimental crane has been built as shown as Figure 61, but it is a small one that makes sure completing some tests in the laboratory, maybe it can be brought to outside to complete or make some test. Some specification of this overhead crane is shown in Table 4:

Table 4 – Specification of Test overhead crane

Specification	Measurement
Size(L*W*H)	1200*200*900mm
Weight	5.0 kg

4.2. Overhead Crane Trolley

The Overhead crane trolley is one part of the overhead crane Figure 27. It is the mechanism that holds the lifting system has moved from the inside out and vice versa.



Figure 27 – Overhead crane

Overhead crane trolley: Cranes lift and lower loads with a hoist that is attached to a trolley [35]. The trolley moves back and forth along a bridge.

The bridge moves along a runway. Some cranes – such as a jib crane [36] – don't have a bridge but still have a hoist attached to a trolley and can move a load in a horizontal direction.

The detailed structure of the trolley is shown in Figure 28.



Figure 28 – The detail structure of trolley

This trolley frame suspends one container by a rope on the bottom of itself, which can catch the loads and goods.

As illustrated in Figure 29, the structure of the trolley in the lab has been designed. It consists of two “U” sheet metals, combined by two screw combinations on each side of the sheet metal. This simple structure can help the payload easy to swing.



Figure 29 – The structure of trolley in the lab

As presented in Figure 30, a board has been installed in the trolley, which can block the light from the lidar sensor and returns in a straight line. This board contributes to the distance measurement and the position detection of the trolley. This is a simple structure, which is easy to reach in the lab under the design. It consists of one wood board and metal stick, combined by screw combination on each side. This simple structure can help Lidar to detect the position of the trolley.



Figure 30 – The wood panel for trolley

4.3. Payload or Container

Payload and container represent the goods, which are heavy and need to be transferred from one side to the other side, for example from shore to ship and vice versa.

In the automatic port, there are lots of containers for loading goods. Its shape is made of iron sheet and is a rectangle with six sides. Therefore, one metal box has been selected to make it like a container, as shown in Figure 31. It is a small one but enough because it needs to combine with the size of the overhead crane, which has been designed in the Lab. Finally, this iron box was selected and was treated as one container in the lab test. Its planes are flat so that it can reflect the microwave by its surface. The basic parameters of the container are to be illustrated in Table 5.



Figure 31 – The container in the lab test

Table 5 – Specification of payload

Specification	Measurement
Size(L*W*H)	90*35*30mm
Weight	100g

This container is suspended under the trolley by a rope, which has 30mm in length. The way how to fix rope in a container is shown in Figure 31. With the movement of the trolley, the container will follow it to sway. There are many cases to affect the motion of payloads, such as acceleration, deceleration, and external disturbances.

4.4. SP25 Millimeter-wave Radars

SP25 is a K-Band radar sensor developed by Nanoradar [28]. It has the advantages of being small size, high sensitivity, light weight, easy to integrate, cost efficient and stable performances. In the implemented system it has the function of range-measurement and collision avoidance. Common applications are related to UAVs, industrial machinery, intelligent lighting, robots, hydrologic monitoring and railway vehicle safety etc.

What is millimeter wave radar?

Millimeter-wave radar is an electronic device that senses objects by transmitting and receiving microwaves. The millimeter-wave has a wavelength between the centimeter wave and the light wave. Compared with the centimeter wave sensor, the millimeter-wave sensor has the characteristics of small volume, lightweight, and high spatial resolution [29].

In 1842, the Austrian physicist Doppler (Doppler, Christian Johann) found the Doppler effect of electromagnetic waves. For nearly two hundred years, people have been adopting the Doppler Effect in radar operations. And then, in Europe and the United States, the use of 24GHz anti-collision radar products in automotive is already very common. Later, Hunan Nanoradar Science and Technology Co., Ltd. set about the R&D of 24GHz millimeter-wave radar sensor earlier. Therefore, it has mature solutions of a millimeter-wave radar sensor system.

SP25 is a light 24GHz radar sensor as shown in Figure 32, 33. It utilizes the frequency difference between the transmitted radio wave and echo wave to measure the distance and velocity of targets. SP25 has the advantages of the lowest power consumption(0.5W) in the same industry, the smallest size (40mm×31mm×6mm), range-measurement of 30m, advanced performances, high cost-effective and integrated peripheral interfaces, which could meet the increasing demands in the range-measurement and collision avoidance in industrial control, UAVs, intelligent lighting, security, robots, and other fields.



Figure 32 – The SP25 radar sensor

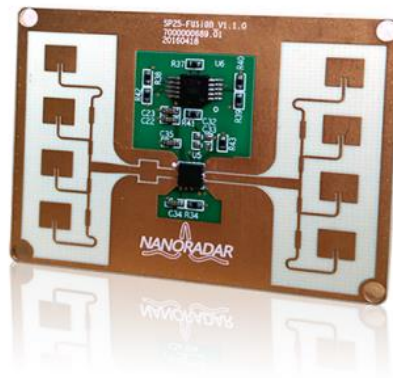


Figure 33 – The SP25 radar sensor in the lab test

This SP25 Millimeter-wave Radar sensor in Figure 33 presents the following specifications [30], (Table 6):

Table 6 – SP25 Specifications

Parameter	Conditions	Min	Typ	Max	Units
System characteristics					
Transmit frequency		24.00		24.20	GHz
Output power(EIRP)			12		dBm
Modulation type		FMCW			
Update rate		50			Hz
Communication interface		UART			
Range-measurement & velocity –measurement characteristics					
Range-measurement range	@0 dBsm	0.1		30	m
Velocity-measurement range		-70		70	m/s
Antenna characteristics					
Beam width/TX	azimuth(-6dB)		100		deg
	elevation(-6dB)		38		deg
Other characteristics					
Supply voltage		4	5	6	V DC
Weight			4		g

Outline dimensions		40x31x6(LxWxH)	mm
--------------------	--	----------------	----

UART interface default rate of Board-level communications is 115200bit / s, and the target refresh rate of 50Hz. With the UART interface, it can quickly integrate with the PC software, such as Labview or other application software, which receives and processes the angle information. In this part, the Matlab is selected to receive sensor data information.

The SP25 sensor interface pins [31] are presented in the following Annex B: B-3 SP25 Specifications.

SP25 sensor data can be acquired and parsed by the "MMW Radar general Management Tool" testing software, which is used to visually display the observation results. It helps us to use the SP25, but in this case, we need to obtain law data from UART.

As shown in Figure 34, with a USB connection to the TTL serial port adapter, to connect PC and SP25, the SP25 can transmit the data to PC [32].

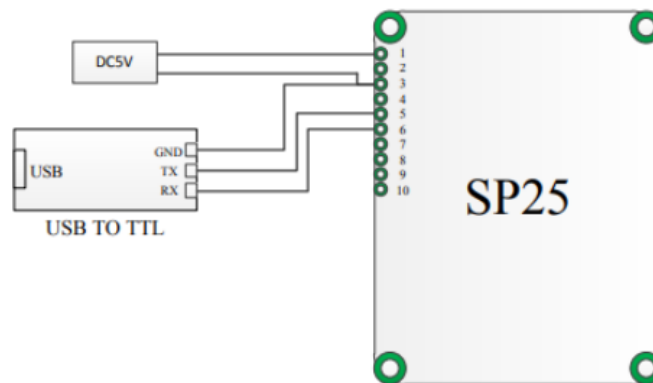


Figure 34 – Connection of SP25 radar to serial port

This type of radar sensor needs that separately supply power from 5V DC stabilized power supply, and do not use the 5Vdc power supply of a USB-TTL adapter. The radome is the radar shell, which is used to protect the radar antenna from the environment.

SP25 radar sensor utilizes a UART-TTL interface with a default transmission rate of 115200 baud, starting with a start sequence and terminating with a termination sequence for each data message. At each data cycle of SP25 (20ms), the message for SP25 system status and target output status would be output. If the field of detected target numbers in

the message of the detected target output status is 1, the target output status message is followed by the target output information message which contains the range, velocity parameter of the target.

PC or the peripheral device is used to configure the SP25 with the same message format, and this message's corresponding message ID is 0x0200.

A complete data message of UART-TTL communication is 14 bytes in Table 7. Each byte of data is unsigned 8bit. The data range is 0 ~ 255 (0 ~ 0xFF). And the format is shown in the following table. Each data message contains a message ID to distinguish between different types of messages in Table 8.

Table 7 – Format of data message

Byte\Bit	7	6	5	4	3	2	1	0
0-1	Start Sequence (2 x Uint8)							
2-3	Message ID (2 x Uint8)							
4-11	Data Payload (8 x Uint8)							
12-13	End Sequence (2 x Uint8)							

The start Sequence is a constant value 0xAAAA, and the Message-ID is defined as follows. The Data Payload is defined according to the Message-ID. The End Sequence is set to 0x5555.

Table 8 – Definition of Message-ID

Byte\Bit	Message ID	Message Name	Comment
1	0x200	Sensor conFiguretion	SP25 conFiguretion
2	0x400	Sensor back	SP25back
3	0x60A	Sensor status	SP25 status
4	0x70B	Target status	Target output status
5	0x70C	Target info	Target output info

The Message-ID is represented by 2 bytes, Byte2 is the low byte, and Byte3 is the high byte. For example, the output of the SP25 message is 0xAA 0xAA | 0x0A 0x06 | Data

Payload | 0x55 0x55, which indicates that the message ID is 0x60A (SP25 system status) and Data Payload is the SP25 system status.

The important information is target output information, which's the format of SP25 is shown in the following table. The start sequence (0xAAAA) and the termination sequence (0x5555) have been omitted from the table. When the radar sensor works normally and detects the target, it outputs the SP25 system status message, and then outputs the target output status message, and finally outputs the target output information message in Table 9.

Table 9 – Format of data message 0x70C

Message ID --- 0x70C					
Signal name	Bit	Resolution	Interval	Type	Comment
Index	0..7	1	0..255	u8	Target ID
Rcs	8..15	1	0..255	u8	The section of radar reflection
RangeH	16..23	1m	0..255	u8	Target distance high 8 bit
RangeL	24..31	1m	0..255	u8	Target distance low 8 bit
Rsvd1	32..39	-	-	u8	u8
VerlH	40..42	1m/s	0..7	u3	Target velocity high 3 bit
Rsvd1	43..45	1	1	u3	-
RollCount	46..47	1	-	u2	SP25 is fixed0
VrelL	48..55	1m/s	0..255	u8	Target velocity low 8 bit
SNR	56..63	1m/s	0..255	u8	SNR

The value of each item in the table is not the true value of the target information. The true value of the target information needs to be calculated through the following relations:

- Index = IndexValue
- Rcs = RcsValue*0.5 – 50
- Range = (RangeHValue*256 + RangeLValue) *0.01
- RollCount = RollCountValue
- Verl = (VrelHValue*256 + VrelLValue) *0.05-35
- SNR = Value-127

The target reflection Radar-Cross Section (RCS), the targets range (Range), and the Signal Noise Ratio (SNR) can be obtained by these calculations, to accurately detect the targets.

4.5. LIDAR Sensor

In order to confirm the position of the trolley, we need to select a sensor to gather the information of the trolley's information. Due to the trolley move on a direct track, we need to select one stable sensor and detect the target in a straight line. However, as we know that the lidar sensor has a good quality for detecting the target in one line, the Lidar sensor was selected for measuring the position of the trolley.

This Lidar Sensor needs that separately supply power from 5V DC stabilized power supply, and do not use 5V power supply of USB—TTL adapter. Thus, this will connect to the Arduino Uno board to provide supply power to this Lidar sensor.

This is the LIDAR-Lite v3 [21], a compact, high-performance optical distance measurement sensor from Garmin™. When space and weight requirements are tight, the LIDAR-Lite v3 soars in Figure 35. The LIDAR-Lite v3 is the ideal solution for drone, robot, or unmanned vehicle applications.



Figure 35 – LIDAR-Lite v3

This device measures distance by calculating the time delay between the transmission of a Near-infrared laser signal and its reception after reflecting off a target. This translates into distance using the known speed of light. Our unique signal processing approach transmits a coded signature and looks for that signature in the return, which allows for highly effective detection with eye-safe laser power levels. Proprietary signal processing techniques are used to achieve high sensitivity, speed, and accuracy in a small, low-power, and low-cost system. There are several specifications, like Physical features of Lidar (Table 10), Electrical features of Lidar (Table 11).

Table 10 – Physical features of Lidar

Specification	Measurement
Size(L*W*H)	20*48*40mm
Weight	22g
Operating temperature	-20 to 60 °C

In the position measurement system for detecting the trolley's location, the Arduino Uno, provide two-level supply power: 3.3V and 5.0V. For this case, the 5.0V can assure the requirement of the supply power, which ask for more than 4.5Vdc and less than 5.5Vdc.

Table 11 – Electrical features of Lidar

Specification	Measurement
Power	5 Vdc nominal 4.5 Vdc min., 5.5 Vdc max.
Current consumption	105 mA idle 135 mA continuous operation

The LIDAR-Lite v3 [23] sensor has a 2-wire, Inter-Integrated Circuit(I2C)-compatible serial interface [22]. It can be connected to an I2C bus as a slave device, under the control of an I2C master device. Support is not provided for 10-bit addressing. The Sensor module has a 7-bit slave address with a default value of 0x62 in hexadecimal notation. The effective 8-bit I2C address is: 0xC4 wire, 0xC5 read. The device will not presently respond to the general call [24].

As Figure 36 shown, the I2C connection diagrams for LIDAR-Lite v3 is present [27]. Table 12 has shown the description of each wire.

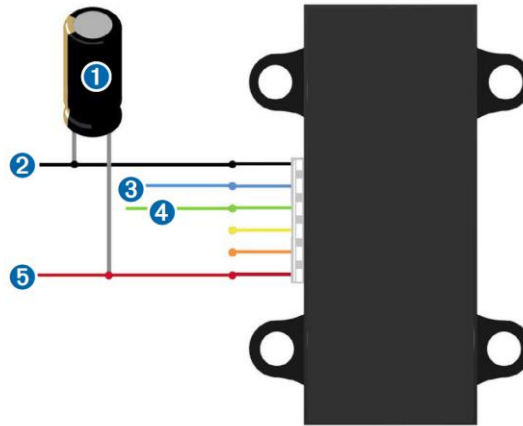


Figure 36 – I2C connection diagrams of Lidar sensor

Table 12 – The description of each pin

Pins	Definition	Range
1	680uf electrolytic capacitor	You must observe the correct polarity when installing the capacitor
2	I2C SDA connection	Black wire
3	I2C SCL connection	Blue wire
4	Power ground (-) connection	Green wire
5	5 Vdc power (+) connection	Red wire the sensor operates at 4.75 through 5.5 Vdc

4.6. Microcontroller - Arduino Uno Rev3

Arduino Uno is a microcontroller board developed by Arduino and based on Atmega328. Electronic devices are becoming compact, flexible, and cheap that can do more function as compared to their predecessors which happened to cover more space turned out costly with the ability to perform fewer functions [33].

Experts always strive to introduce innovation in automation that requires minimum effort and gives maximum output. The microcontroller was introduced in the electronics industry with the purpose of making our tasks easy which comes with even a remote connection with automation in any way. Microcontrollers are widely used in embedded systems and make devices work according to our needs and requirements.

Arduino Uno is a very valuable addition to the electronics that consists of a USB interface, 14 digital I/O pins, 6 analog pins, an Atmega328 microcontroller. It also supports serial communication using Tx and Rx pins. There are many versions of Arduino boards introduced in the market like Arduino Uno, Arduino Due, Arduino Leonardo, and Arduino Mega [33]; however, the most common versions are Arduino Uno and Arduino Mega.



Figure 37 – Arduino Uno Rev3

Arduino Uno Rev3 in Figure 37 comes with a wide range of applications [33]. A larger number of people are using Arduino boards for developing sensors and instruments that are used in scientific research. Therefore, in this project, Arduino Uno Rev3 [34] will be used to obtain, decode, process, and output the distance data from the Lidar sensor, and then transmitting the result of the distance to the PC terminal. The Arduino Uno Rev3 has some interfaces, such as UART and I2C. UART will connect the Arduino Uno Rev3 to

PC to upload the result of position, while I2C will establish the communication belt between Arduino Uno Rev3 and the Lidar Lite sensor. The Arduino Uno Rev3 could send some control commands to configure or read registers in the Lidar sensor.

When the Arduino Uno Rev3 connect to the DC power, this microcontroller can provide two range of DC power respectively 3.3Vdc and 5.0Vdc. Therefore, the Arduino Uno Rev3 can provide supply power to the Lidar Lite sensor rather than need other supply power. More information in AnnexB: B-4 Arduino Uno Rev3 specifications.

Eventually, this hardware, overhead crane, trolley, payload(container), SP25 Radar sensor, Lidar Lite sensor, and Arduino Uno Rve3, are constituted to build a completed system model.

Chapter 5 – Software

For the hardware listed in the previous chapter to function properly in our system, specific software must be implemented. This chapter focuses on discussing the following topics:

- Arduino IDE;
- Matlab Simulink Simscape;
- Matlab Software

Every component attached to the Arduino will be programmed using the Arduino IDE software, by C/C++.

5.1. Arduino IDE

5.1.1. Introduction of Arduino IDE

Arduino IDE is open-source software dedicated to development in Arduino boards, such as Arduino Uno, Arduino Mega, and in our case, Arduino Nano. This is a cross-platform application, meaning it can be developed in different OS's, such as Windows, Linux, and macOS.

There are also a lot of products that claim to be “original” Arduino, using our graphics and branding, but provide no contributions back to Arduino for the development of the software and running the website. The point of this software is to upload a program into the Arduino's microcontroller's flash memory, with the possibility of changing said code by uploading it again if necessary. It also contains a core library with basic methods, such as setting pin modes to high or low and reading digital and analog pins for instance. This is also known as firmware.

5.1.2. Basic functions for an application

In order to develop an application, a sketch should be created first, containing two mandatory methods:

- `setup()` – only runs once when the board is powered, or the reset button is pressed;
- `loop()` – runs the method continuously without stopping.

The first function, `setup()`, is called when a sketch starts and it is used to initialize variables, pin modes, and libraries.

The `loop()` function, on the other hand, does exactly what the name suggests, looping consecutively every few seconds, defined by a `delay(time)` function, with time being in milliseconds.

In this project, the Arduino Uno Rev3 need to configure some parameters, and then to detect or measure the distance of the trolley. As the flow chart for the whole Lidar to detect distance shown as following in Figure 38:

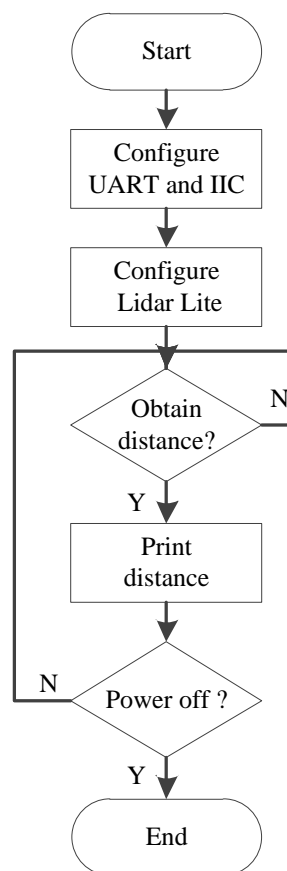


Figure 38 –The flow chart for whole Lidar to detect distance.

When the Arduino was provided the supply power, it must initialize the serial connection to display the model for showing the value of distance. Secondly, the communication line for IIC also needs to configure to connect the Lidar Lite to the Arduino Uno, assuring the correction of communication between Lidar Lite and Arduino Uno. After the connection, the Arduino Uno will start to read the byte value of distance information from the Lidar Lite's register, where is used to save the value of distance. When the Arduino Uno received data, it is necessary to check the effectiveness of it. If

the value of the distance is invalid, the Arduino Uno will start to read again until obtaining the valid distance data. The result of distance (cm) will display on the serial monitor, as shown in Figure 39.

```

10:31:02.842 -> 76
10:31:02.842 -> 77
10:31:02.842 -> 76
10:31:02.842 -> 77
10:31:02.880 -> 75
10:31:02.880 -> 77
10:31:02.880 -> 76
10:31:02.880 -> 76
10:31:02.880 -> 75
10:31:02.880 -> 76
10:31:02.880 -> 77
10:31:02.880 -> 76
10:31:02.880 -> 76
10:31:02.880 -> 76
10:31:02.880 -> 76
10:31:02.880 -> 75
10:31:02.927 -> 77

```

Figure 39 –The result of distance for trolley.

If the supply power doesn't cut, the loop() function will continue to obtain the real-time distance, which is good for monitoring the state of the trolley in the overhead crane system.

As shown in Figure 40, this flow chart represents the process to configure work mode.

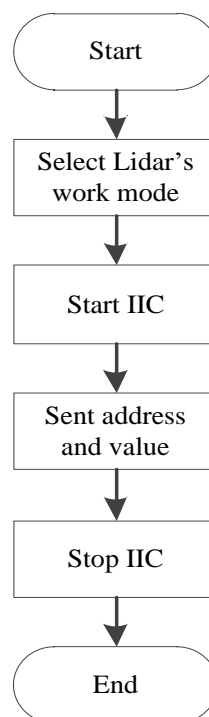


Figure 40 – The flow chart for configuring lidar's work mode.

At first, every sensor has some special work mode, thus, this Lidar sensor is not an exception. There are six work modes for this Lidar sensor, including:

- Default mode, balanced performance;
- Short range, high speed;
- Default range, higher speed short range;
- Maximum range;
- High sensitivity detection, high erroneous measurements;
- Low sensitivity detection, low erroneous measurements;

After finishing the selection of work mode, it needs to start IIC to transfer configuration information to the register in the Lidar sensor. Due to every register has its own independent address, the register's address and configuration information should be sent to the IIC device together. Finally, the mode configuration is completed.

How about the Arduino Uno to read the values of distance from the lidar sensor? There is a flow chart shown in Figure 41.

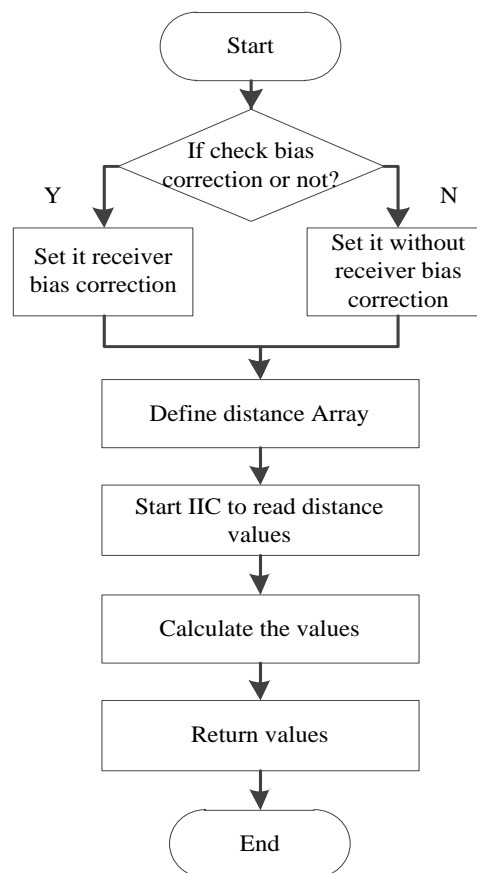


Figure 41 – The flow chart about the detail of distance reading.

At first, when starting to execute the process of reading distance, it should set the receiver bias correction for the acquisition and correlation processing. If set to false, measurements will be faster. Receiver bias correction must be performed periodically. So, this parameter will be set true, because it needs the receiver bias correction. Due to the value of distance was saved at two bytes, it is needed to define an array, such as “byte distanceArray[2]”. So far, the IIC is always in a dormant state and it needs to be activated to transfer data. when the “distanceArray[2]” fulfil with the value, let’s convert the “distanceArray[2]” to the final value by using “int distance = (distanceArray[0] << 8) + distanceArray[1];” and return the distance value to the main function.

5.2. Matlab Simulink Simscape

Simscape [51] is the MathWorks Language of physical modeling. This tool supports the ability to model multi-domain systems. A significant aspect of Simscape is that the connections between components are bidirectional, and these real physical connections also have individual units. They need to add the components to the system to build the whole system model.

Simscape add-on products provide more complex components and analysis capabilities. With Simscape, you build physical component models based on physical connections that directly integrate with block diagrams and other modeling paradigms. Therefore, Simscape enables you to rapidly create models of physical systems within the Simulink environment. This modeling software can provide us with powerful modeling functions and can meet all our modeling needs.

Simscape Multibody [52] allows to 3D rigid body dynamics of a system while providing a 3D animation of the system response. In overhead crane modeling, the motion of the trolley can be easy to simulate and visualize system dynamics. It can also be used to design a subsystem, which is useful to design one time and use many times. Figure 42 shows the Simscape product family with the platform and add-on products.



Figure 42 – Simscape product family

In order to build a Simulink system for the overhead crane, it needs 3D modeling software and can provide some blocks for adjusting parameters and outputting variables. According to this demand, the Matlab Simulink Simscape can provide a simulation platform with a completed function.

At the same time, the Simscape can reduce the visual complexity of a Simulink model.

In the Simscape development environment, Simscape helps us develop control systems and test system-level performance. The overhead crane can be created by custom component models using the MATLAB based Simscape language, which enables text-based authoring of physical modeling components, domains, and libraries. The overhead crane can be parameterized by using MATLAB variables and expressions, and design control systems for this physical system in Simulink.

To deploy the overhead crane models like other simulation environments, including hardware-in-the-loop (HIL) systems, Simscape is a good option. Because it provides the Simscape Multibody to researcher and developer to design physical model. When they have an idea to create a new project or product, they could use the Simscape Multibody to build the model and observe the performance of them. More information in AnnexB: B-1 Multibody model anatomy.

5.3. MATLAB

Matlab [53] is the language of technical computing, Millions of engineers and scientists worldwide use MATLAB to analyze and design the systems and products transforming our world. Matlab provides tools to run our project to obtain distance data and analyze the result.

5.3.1. Why choose m-file?

An m-file is a simple text file where you can place MATLAB commands. When the file is run, Matlab reads the commands and executes them exactly as it would if you had typed each command sequentially at the MATLAB prompt. Due to there are a lot of commands needed to write, m-files will be helpful and almost necessary in these cases.

5.3.2. The analysis process for container data

In this part, a new script (.m file) has been created. The main purpose of the new script is going to deal with messages from the radar sensor, furthermore analysis of these data. As shown as a flow chart in Figure 43, there are some steps for the message processing.

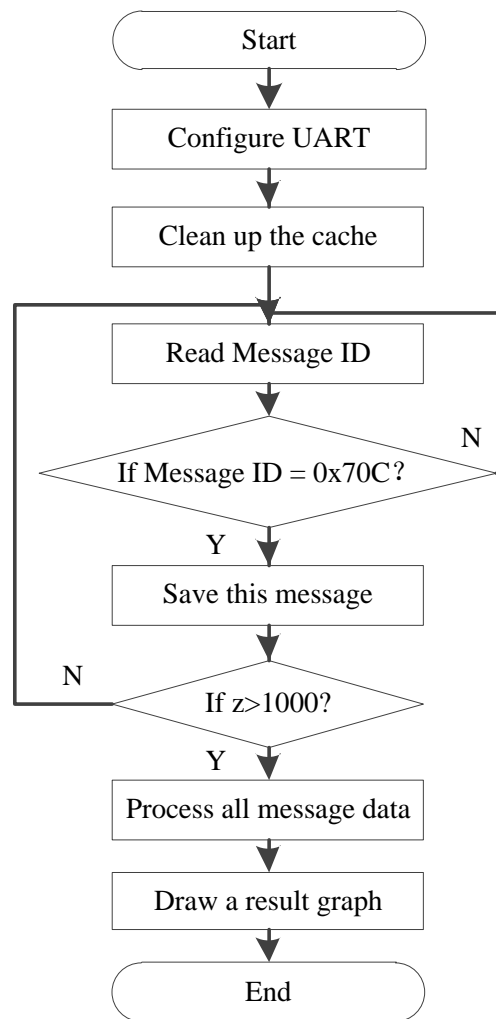


Figure 43 – Flow chart for the message ID = 0x70C processing.

When the experiment starts a data collection, the first thing that should be done is that and configuring UART, which means that creating a UART control variable in the Matlab to establish the connection between PC and Radar sensor. Due to the Radar sensor always output state message, the cache space has been fulfilled with useless information. Thus, before reading a real-time message, the cache should be clear up.

After this, the demo starts to read the message from the cache. It is necessary to judge the message ID, which is a valid message. if met the 0x70C message during the loop process, this message should be saved into the message matrix and start to wait next message. If the total data of messages over the defined amount, the data collection process will be suspended.

According to the message format, all these message data will be decoded to relevant variables. These variables include the distance, velocity, and a number of targets. Finally, the distance graph has been drawn and display.

Chapter 6 – Simulation Results and Discussions

In this section, some simulations are performed to verify the efficiency of the proposed method. However, In the whole simulation, the physical system of the overhead crane has been built by using Simscape Multibody [52]. The overhead crane is run through some simple tests to explore requirements for the actuator and see how the entire system behaves.

6.1. Simscape Multibody Recap

As above mentioned, the Simscape Multibody [52] provides a multibody simulation environment for 3D mechanical systems, which can design robots, vehicle suspensions, and aircraft landing gear. This Simscape Multibody has many useful blocks, including joints, constraints, force elements, and sensors. An automatically generated 3D animation lets you visualize the dynamic state of the physical system, as shown in Figure 44.

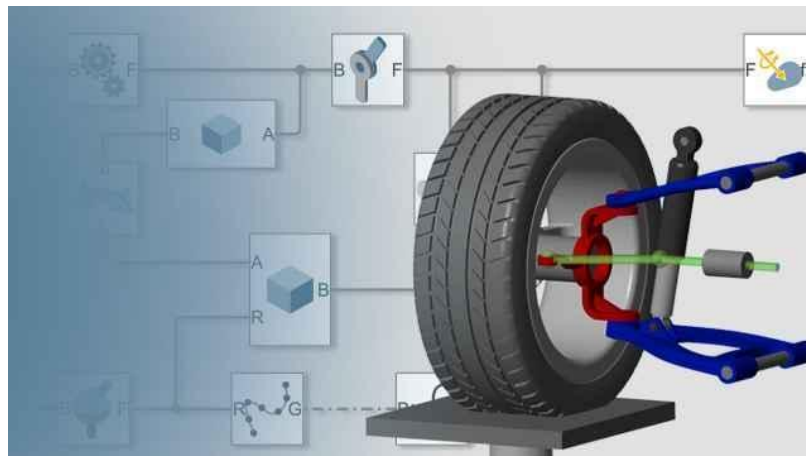


Figure 44 – 3D Animation

6.2. Simulation System

The chosen simulator for the theory validation in this project was Simscape Multibody. It provides a multibody simulation environment for 3D mechanical systems, such as robots, vehicle suspensions. It can model multibody systems using blocks representing bodies, joints, constraints, force elements, and sensors. One example has been shown in AnnexB B-2 A multibody model example

According to the basic relationship of experimental equipment, one of the 3D mechanical systems for the overhead cranes (Figure 45) has been built. This is a dynamic Simulink and visual system model shown in the Matlab, which helps us easy to analyze performance and possible improvement.

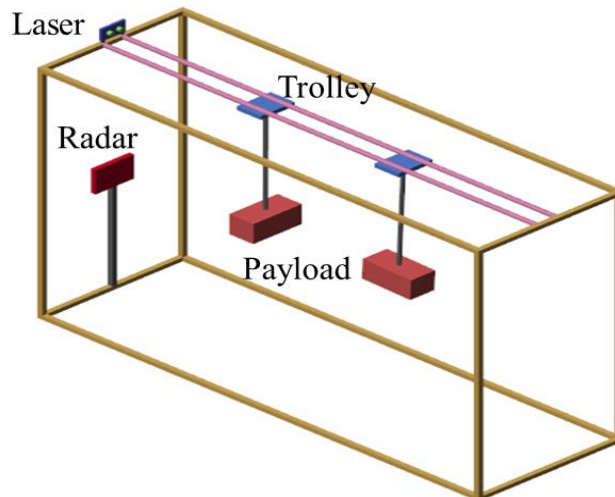


Figure 45 – The physical model of overhead crane system

6.2.1. Overhead crane model structure

As shown in Figure 46, this overhead crane model structure has been designed by Simscape Multibody, and this simulation system consists of some basic parts and some important subsystems, as following:

- Framework – Overhead crane body
- Lidar sensor (Figure 47);
- Radar sensor (Figure 48);
- Moving payload (Figure 49);
- Fixed payload (Figure 50);

The framework of the overhead crane body is the basic shelves of the crane body, which will be used to put or install the sensor or trolley. The lidar sensor was installed on the top of the crane at the one side of the track. The lidar sensor can output the distance of the trolley. The radar sensor was installed on the bottom of the overhead crane, and it was used to measure the distance between the payload target and the radar sensor. At the same time, two cases of motion for payload has been considered in this project, thus, two subsystems about two types of the payload have been designed for overhead crane system. The subsystem of moving payload represents the trolley under a position control signal, while the subsystem of fixed payload represents the trolley affected by the external disturbance, such as storm and heavy rain.

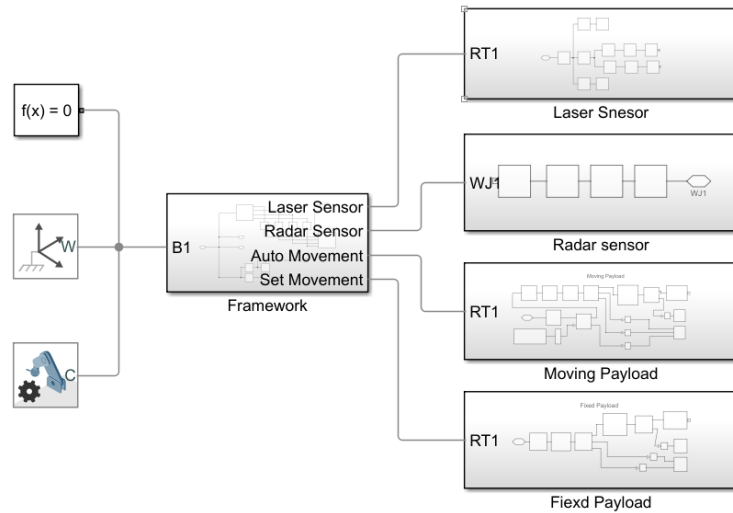


Figure 46 – The structure of overhead crane model

6.2.2. Subsystems description

The first subsystem is the Lidar sensor. According to the description of the datasheet of Lidar Lite V3, the diagram of the Lidar sensor has been designed, as shown in Figure 48. Its function is that detecting the position of the trolley between the trolley and the Lidar sensor. This Lidar sensor consists of Laser Body, Laser transmitter (TX), and laser receiver (RX).

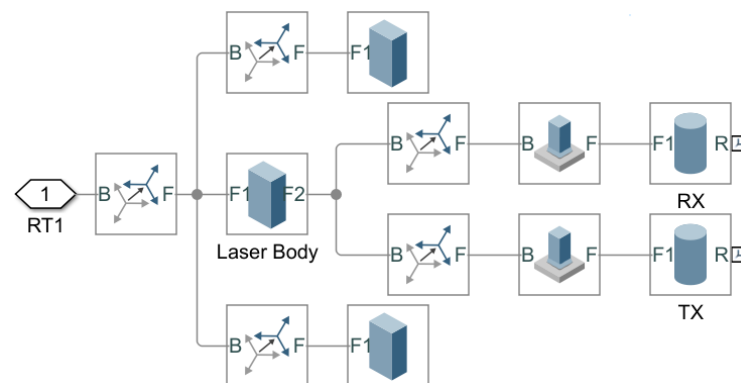


Figure 47 – The diagram of Lidar sensor

The second subsystem is the Radar sensor. According to the description of radar’s features, the diagram of the radar sensor has been designed by Simscape Multibody in simulation, as shown in Figure 49. It represents one type of radar sensor, which is used to measure the distance between payload and radar sensor.



Figure 48 – The diagram of radar sensor

The third subsystem is moving payload. The moving payload considers the situation of the trolley controlled by a position control signal along the track. The diagram of the moving payload has been designed, as shown in Figure 50. It consists of position signal, rope, and payload.

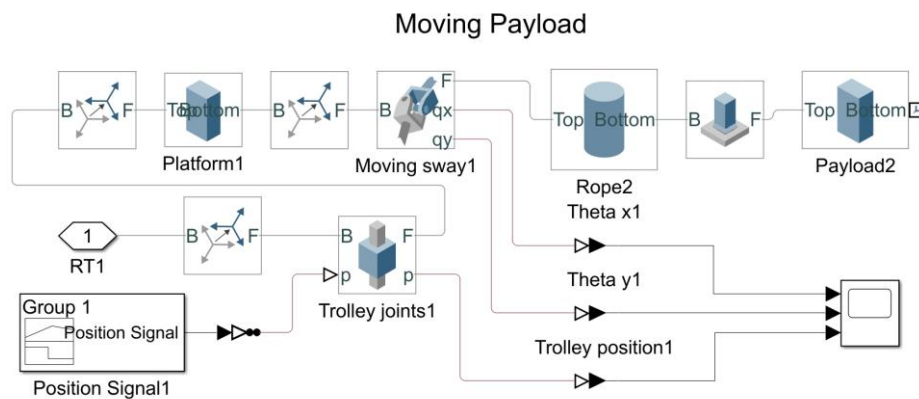


Figure 49 – The diagram of moving payload

The last subsystem is Fixed payload. The Fixed payload mainly consider that payload or container was affected by the external disturbance, made the payload to swaying. Therefore, the diagram of moving payload has been designed, as shown in Figure 51. It consists of trolley, rope and payload.

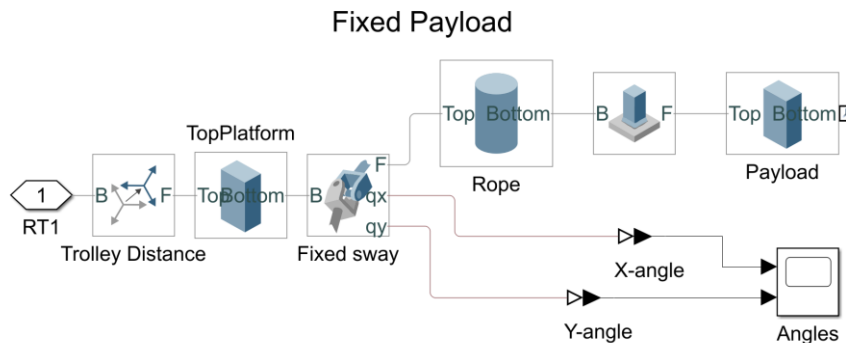


Figure 50 – The diagram of fixed payload

It is the existence of these subsystems that constitute the entire overhead crane system. If some parts occur error, we can directly check with the subsystem. These subsystems represent the feature of the overhead crane. The next section will talk about the results of each situation.

6.3. Simulation Results

6.3.1. The fixed payload

This is one case of the motion of the payload. There are many external disturbances, which will affect the container under stationary conditions. Therefore, this fixed payload is considered in this simulation part. Assuming that the initial angle is 5 deg for the fixed payload test and the trolley will be set at one position. The dynamic picture of the fixed payload is shown as following Figure 51. As mentioned in the assumptions, the trolley (blue block) has been fixed in the track at 0.4 m, and the initial position of the payload will be lanced when the test starts to run.

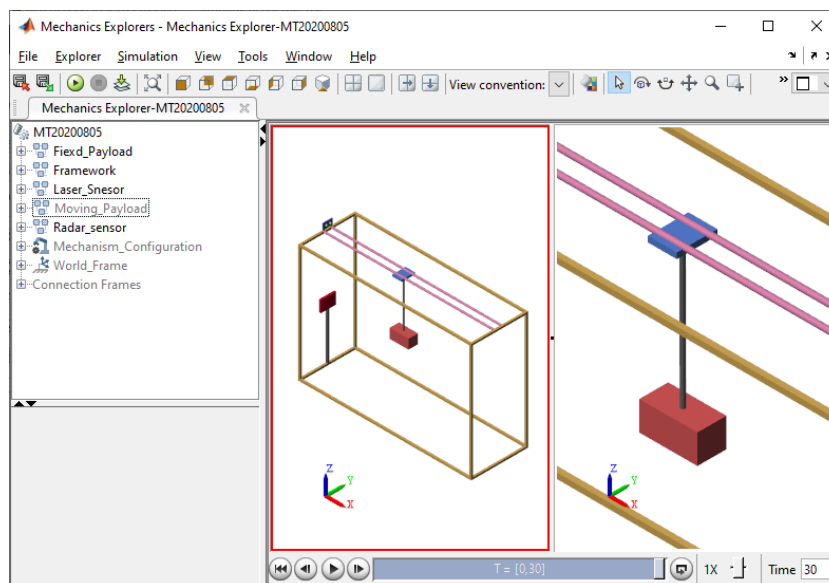


Figure 51 – The dynamic picture of fixed payload

The testing result for the first case of the payload has been output and displayed in Figure 52. It shows the value of the angle, angular velocity, and angular acceleration of the junction between the trolley and the rope.

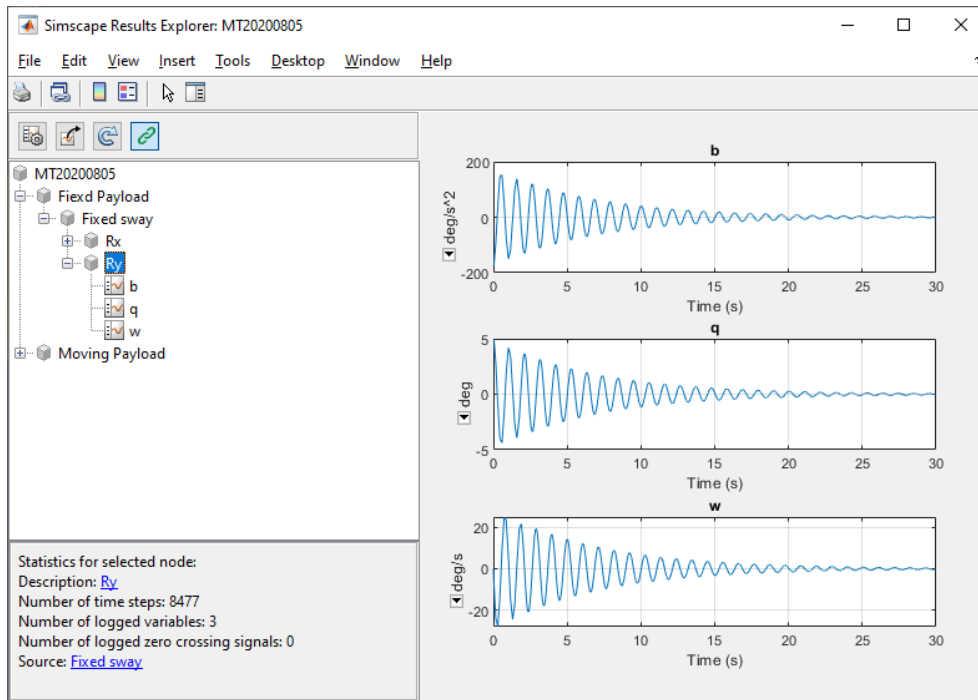


Figure 52 – The graph result from fixed payload

In this simulation model, it is hard to directly obtain the distance between the target and the radar sensor, because the spatial coordinate position of each block cannot be obtained directly from the output. Thus, this distance should have been calculated by the relationship of coordinates in the simulation model.

We set the trolley at one fixed position and change the length of the rope. $d=60\text{cm}$, $l=45\text{cm}$, 35cm . The simulation results of the sway angle are shown below in Figure 53, 54. There are some curve labels that should be explained in the figure. The curve label of Sway Angle (M) represents the sway angle from the physical overhead crane system in the simulation. The label- “Distance (r_2)”- represents the distance between container(object, or payload) and radar sensor, the distance (r_2) has been calculated as above mentioned in Table 2. The label- SwayAngle(C)- represents the calculated sway angle of payload, which was calculated according to the proposed method by Equation (4).

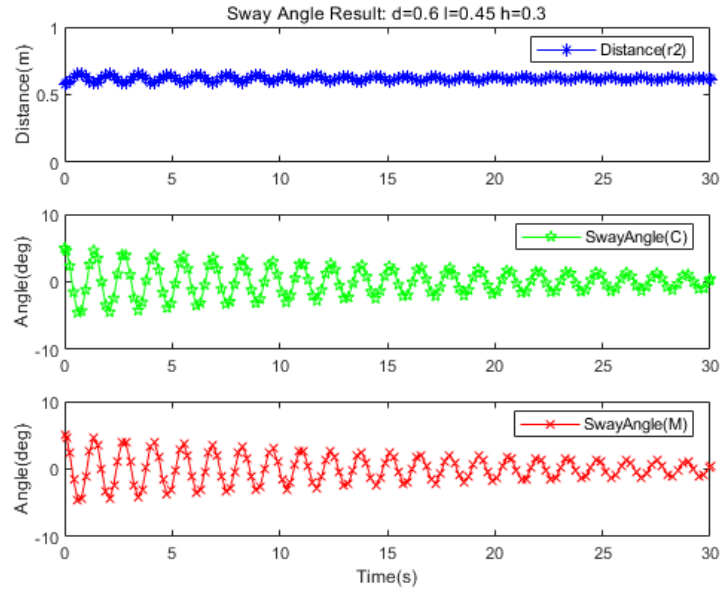


Figure 53 – The evolution of distance and sway angle for the particular case of Distance of trolley, $d=0.6m$, Length of rope, $l=0.45m$ (simulation)

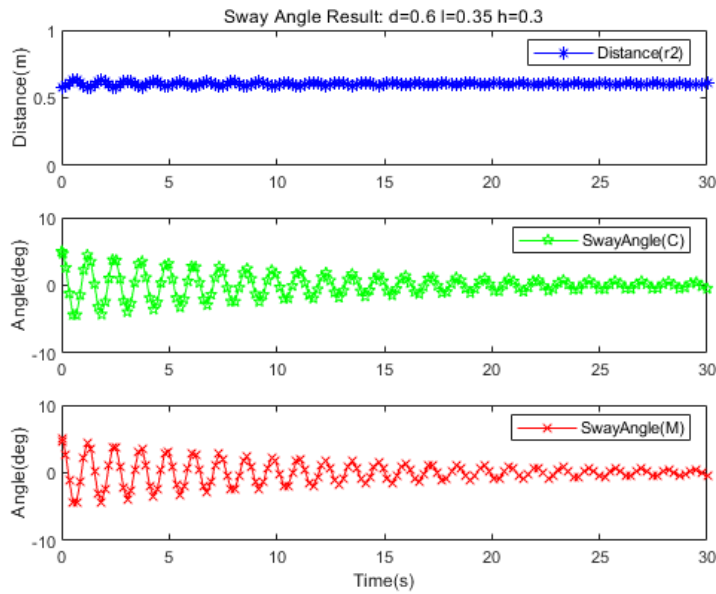


Figure 54 –The evolution of distance, sway angle for the particular case of Distance of trolley, $d=0.6m$, Length of rope, $l=0.35m$ (simulation)

The period of data collection for the simulation system is $T=30$ s. From Figure 53, 54, it can be known that the fluctuation range depends on the length of the rope. The Calculation method of sway angle has been verified by this simulation.

After the first simulation, the condition has been changed, as shown in Figure 55, 56. The rope length was set with the value as $l=0.25$, and the distance of the trolley's position was set with a different value as $d = 0.5, 0.4$. The simulation result of the second test displayed in Figure 55, 56.

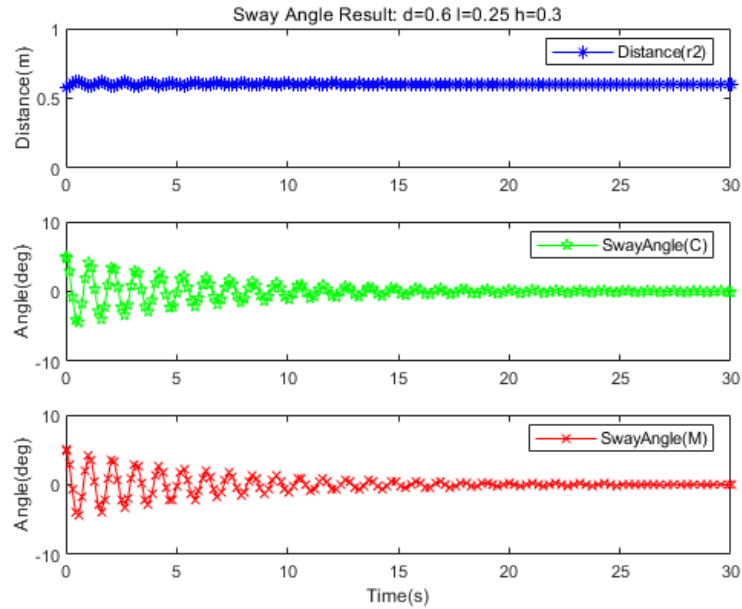


Figure 55 – The evolution of distance and sway angle for the particular case of Distance of trolley, $d=0.6m$, Length of rope, $l=0.25m$ (simulation)

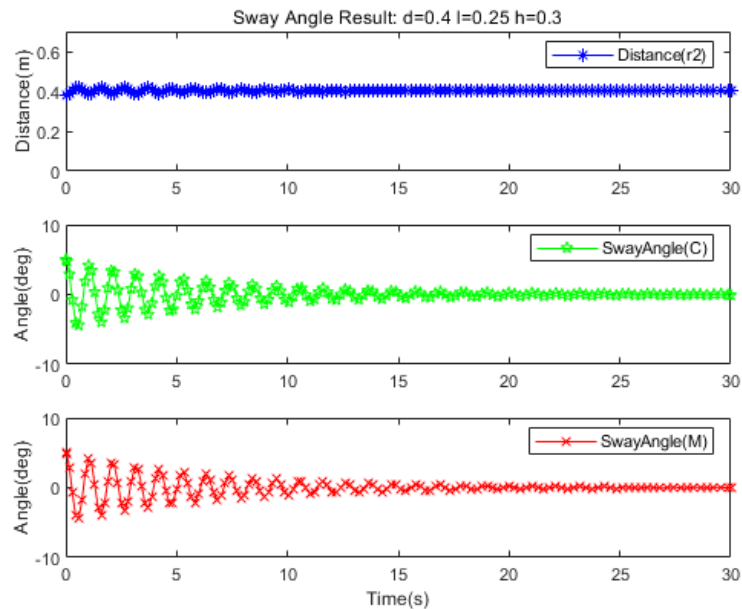


Figure 56 – The evolution of distance and sway angle for the particular case of Distance of trolley, $d=0.4m$, Length of rope, $l=0.35m$ (simulation)

In Figures 55, 56, it can be observed that the fluctuation range is similar because the length of the rope is different. The distance has different, due to the distance of the fixed position of the trolley.

In this second group of simulation results, the calculation method of angle is verified. The sway angle will be correct if the accuracy of measurement data has been guaranteed.

6.3.2. The moving payload

Regarding other cases of motion of the trolley in the overhead crane system, the moving payload, which includes the operation of acceleration or deceleration during the transportation of goods, has been considered in this part. The experimental test for moving payload has been launched and implemented in the Simscape Multibody. Therefore, the physical simulation model for moving payload was established, as shown as following Figure 57.

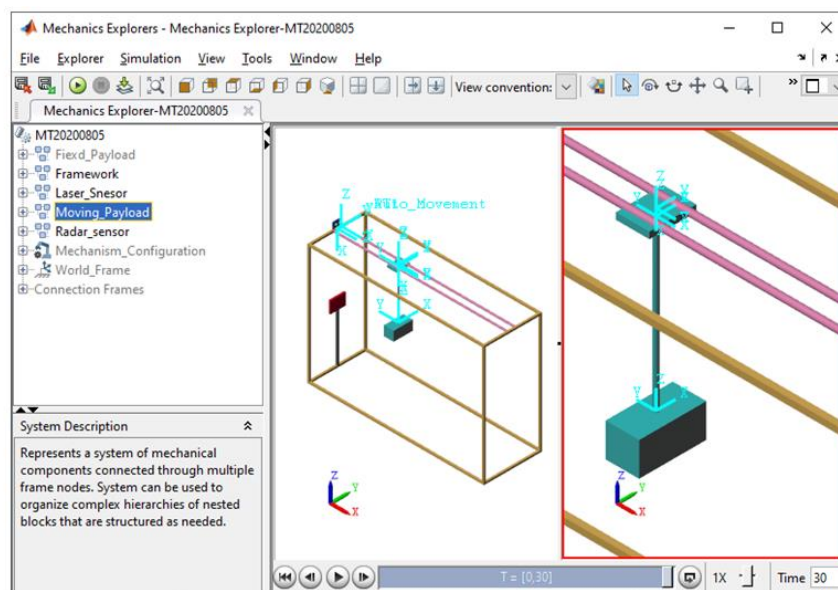


Figure 57 – The dynamic picture of moving payload

For this case, the position of the trolley must be changed during the test. This is said that the trolley should run on the track. Therefore, given a position signal for the trolley; and use two differentiators to convert this signal into an acceleration signal, and this acceleration signal will act on the car and make the car move.

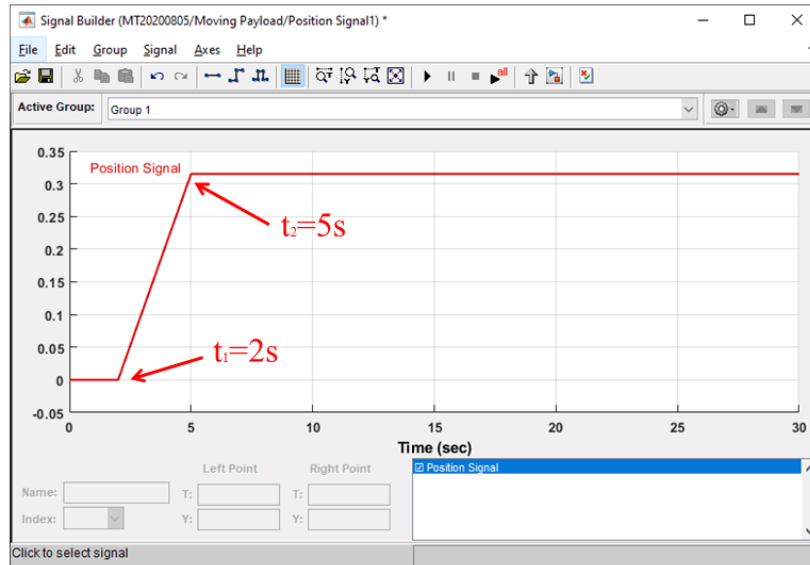


Figure 58 – A given position signal for moving payload

Therefore, the position signal has been drawn as shown in Figure 58. The trolley will follow this signal to keep moving. And then, assuming that the initial swing angle is 0 deg. According to the position signal, the initial position of the trolley is 0m. When the time reaches $t_1=2$ second, the trolley starts to complete the horizontal movement along the track; when time reaches $t_2=5$ second, the trolley will keep at one position 0.32m. During this period of motion, with the movement of the trolley, the payload starts to sway at the same time. Finally, the output information of angle, angular velocity, and angular acceleration is shown in Figure 59.

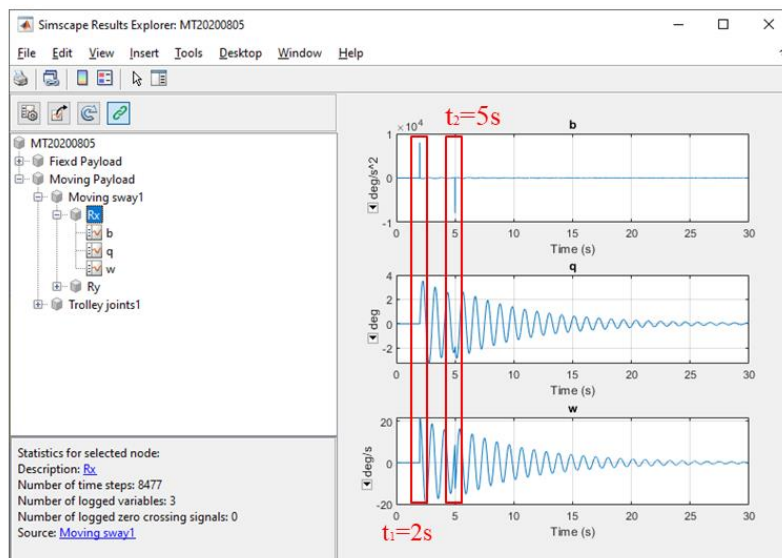


Figure 59 – The result of angle information for moving payload

These two cases of motion are common operations, which always occur in the port and factories when the overhead crane system works moving the heavy goods from one side to another side. If we know the laws or rules of the movement about the huge overhead crane, the overhead crane will be easy to control. When the trolley was provided with a control signal, such as an acceleration signal or a deceleration signal, its motion will be changed.

Chapter 7 – Experimental Results and Discussions

This chapter focuses on demonstrating the experimental results associated with the overhead crane system tests in the Laboratory. The emulated crane has been built to solve the requirement of the experiment. The first phase of testing is that obtaining sensor data from the SP25 mm-Wave Radar, and these imported data will be processed and analyzed in Matlab simulation. The detail of the data process will present in 7.1. The second phase will show the test results. Therefore, some experiments are performed in this chapter to verify the efficiency of the proposed method for measuring the sway angle of containers.

7.1. Obtain the Data from the SP25 mm-Wave Radar

To validate the proposed method, an experimental system prototype was built in Figure 60. The payload was suspended under the trolley by a rope, which locates between the trolley and payload. The mm-Wave radar sensor is fixed on other sides, which contributes to detecting distance. The Laser sensor has been installed on top of the crane, which is used to detect the position of the trolley. However, in order to simplify this overhead crane, the friction is ignored in this experiment. As for simulating the real condition of sway angle, the payload is pulled up by hands and releases, and then the radar sensor will start detecting. The distance measurement was carried out by using SP25 millimeter-wave radar. The SP25 is a light 24GHz radar sensor. It utilizes the frequency difference of microwave to measure the distance and velocity of the payload.

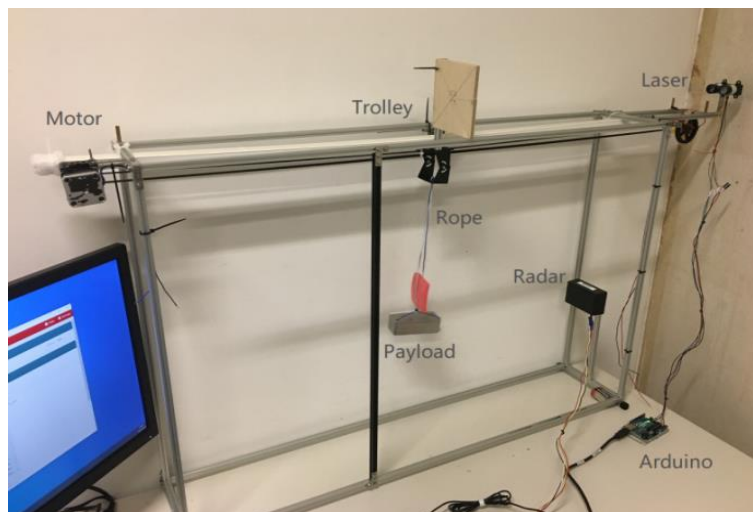


Figure 60 – Experimental setup

In order to import the sensor data to the Matlab, some Matlab code has been implemented as shown in Figure 61, 62:

```

%Initialize the serial port (1)
RadarObj = serialport('COM4', 115200); %Set the serial port parameters
configureTerminator(RadarObj,85,170); %Set ending symbol
flush(RadarObj); %Clear input and output cache
pause(1);
flush(RadarObj); %Clear input and output cache

%Set data configuration (2)
N=100; %Read N data at one time
data=read(RadarObj,N,"uint8"); %Read data from serial port
z = 0; %Set the index of the data
TotalNumber=1000; %Set the total number of data
test1=read(RadarObj,1,"uint8"); %Continuous test data

```

Figure 61 – Initial configurations for serial port using Matlab

The steps of the performed tests are following described:

Step1- Initialize the serial port (1). This is an important step. If the configuration is incorrect, such as the port number and the band rate, the radar data can not obtain from the Bus of the serial port. Therefore, we set the “COM4”, “115200” and ending symbol.

Step2- Set data configuration (2). This step for getting the amount of radar data at one demo test. Meanwhile, this simulation demo read the first test1 data from cache for recognizing the whole data frame.

```

%Read data from radar sensor (3)
while(z < TotalNumber)
    test2=read(RadarObj,1,"uint8"); %Continuous test data
    if(test1==12&&test2==7) %Determine whether to meet "0x70c"
        z = z+1 %Count the time of detection +1;
        data2(z,:) = read(RadarObj,9,"uint8"); %Extract data from cache
    else
        test1=test2;
    end
end

%Process those radar sensor (4)
Index = data2(:,1);
Rcs = data2(:,2).*0.5 - 50 ;
%Calculate the value of distance of target %Column4,5
Range = (data2(:,3).*256 +data2(:,4)).*0.01 ;
RollCount = bitshift(bitand(data2(:,6),192),-6);
%Calculate the value of velocity of target %Column6,7
Ver1 = (bitand(data2(:,6),7)*256 + data2(:,7)) .*0.05-35 ;
SNR = data2(:,8) - 127 ;

```

Figure 62 – Data processings for radar sensor

Step3- Read data from a radar sensor (3). As shown in Figure 62, this step includes a condition check for the message ID, loop processing, and data storage. If the set conditions are met, the sensor data will be saved in the Matlab variable matrix. If the total number “z” reaches the set value, the loop will be stopped.

Step4- Process that radar sensor data (4). This step is to convert the valid data because the initial data is not the real value. Therefore, according to the message analysis rules as mentioned in Table 1 – Format of the data message, we can get the real value for each parameter, as following:

- $\text{Index} = \text{IndexValue}$
- $\text{Rcs} = \text{RcsValue} * 0.5 - 50$
- $\text{Range} = (\text{RangeHValue} * 256 + \text{RangeLValue}) * 0.01$
- $\text{RollCount} = \text{RollCountValue}$
- $\text{Verl} = (\text{VrelHValue} * 256 + \text{VrelLValue}) * 0.05 - 35$
- $\text{SNR} = \text{Value} - 127$

7.2. Testing Results of SP25 mm-Wave Radar

Regarding the geometric setup of the implemented system, the length of the Rope is $l=0.32\text{m}$; the position of the Radar sensor is $h=0.35\text{m}$; the initial position of the Trolley is $d=0.49\text{m}$. During the implemented experimental protocol, the distance will be changed associated with load motion during the operation.

The results of the calculated sway angle and distance are shown in Figure 63. The red line represents the calculated sway angle. The brown line represents the distance between the payload and a radar sensor.

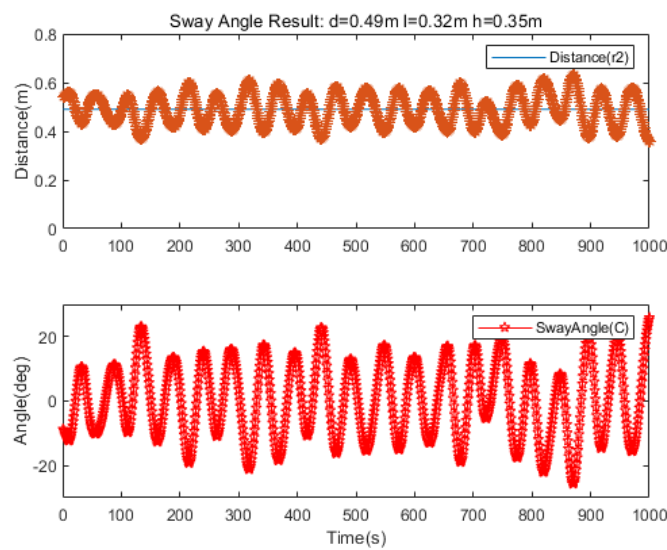


Figure 63 – Experimental results, for the distance of trolley $d=0.49\text{m}$.

From the Figure 63, the distance of payload fluctuates around the distance $d=0.56$, and it is real performance to reflect the real state of overhead crane.

Chapter 8 – Conclusions and Future Work

8.1. Conclusions

In this program, we have developed an overhead crane framework for a radar detection system in the Lab. At the same time, the simulation model for the overhead crane system has been established in the matlab.

An mm-wave radar sensor was used to measure payload distances and sway angles for containers in an overhead crane environment. When those contactless sensors have been installed, it not only improves the performance of detection but also decreases physical collision and of them, thereby extending the service life of these sensors and reducing maintenance fees. The mm-Wave sensor also provides the remote sensing technology, which will improve the overhead crane system functionalities including the measurement of the sway angle but also the positioning of the trolley.

The obtained simulation results are proving the proposed method capabilities. The method can be able to provide an indication for performance of detection. The proposed method provides single target detection that can be considered a limitation considering the real scenarios that imply several targets connected to payload and trolley, which will increase challenges to identify the payload. The method may be improved, to serve for multiple target scenario, considering data fusion algorithms, such as calculating multi-sensor, that can assure accurate payload target recognition.

The experimental results show some of the realistic condition of the overhead crane. The used radar in the realistic environment can detect a few targets at the same time, therefore, there are some unregular movements in the results, which means that some detected distances far beyond the position value of the trolley. The used filtering algorithm for the test data is helping to select and delete invalid data.

The Simscape Multibody that was used in this project represents a simulation platform able to simulate the physical system before we set up the new product. It provides lots of convenient function to us to analyze the performance of the physical system, such as constraint force, constraint torque, and inertia. In actual practice, the physical performance is ever-changing, so it is difficult to grasp its certain laws, so it is necessary to use Simulation Simscape Multibody to consider these technical issues. In the simulation function, there are other functional models, including Generic simscape, Electrical, Electrical Three-Phase, Gas, and others.

The remote sensing technology that was used in this project gives us an example to build a system to detect or measure some contact-less target in some extreme environment, such as a port with a heavy storm. The remote radar sensor provides the function of long-range distance detection, which is good for achieving a goal or requirement of remote detect distance.

One of my paper have been uploaded to 2021 Telecoms Conference (ConfTELE), in Annex C. The title is that “*Microwave Radar Based Estimation of the Sway Angle of Payload in Overhead Crane System*”.

8.2. Future Work

This program had many challenges and as it usually occurs in these lengthy projects, it has many parts that can be improved in the future, such as the following:

Future work will be represented by the development of new software components associated with mm-Wave Radar signal processing including new filter algorithms.

New filtering processes (like noise filter, blur filter, high-pass filter, low-pass filter, band-pass filter, etc.) should be designed and applied to this measurement system to improve the performance of the system in the case of recognizing the target.

At present, there is just one radar sensor installed in the overhead crane system. However, we can consider a few radars and let them work together at the same time, which is called multi-sensor fusion technologies, as shown in Figure 64. As for sensor fusion technologies, there has been a lot of research on intelligent ground vehicles, where obstacle detection is one of the key aspects of vehicle driving [37]. Thus, multi-sensors are the key to the perception of the outside world in the automated driving system and whose cooperation performance directly determines the safety of automated driving vehicles [38].

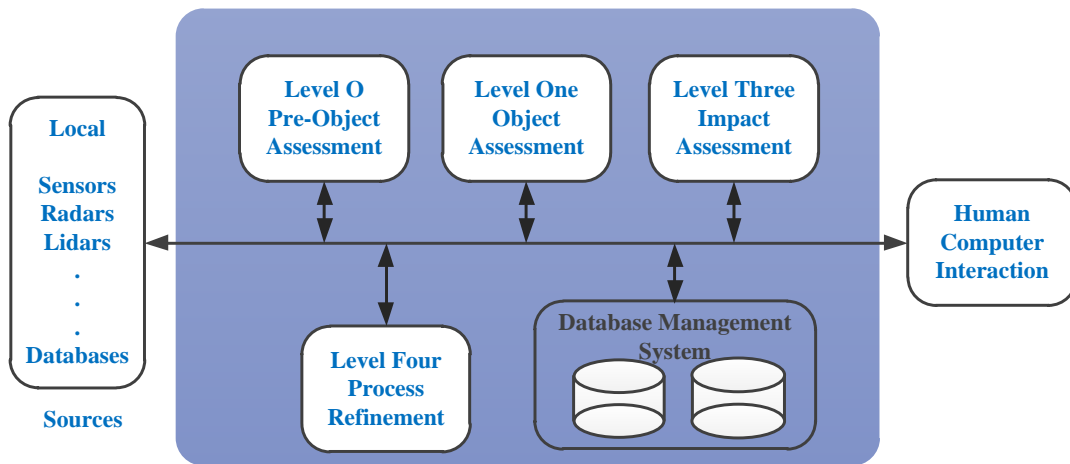


Figure 64 – The diagram for sensor fusion technologies.

Additionally, after new filtering processes and new sensor fusion technology will have been proposed, new experimental tests will be carried out in the actual port, like Shanghai Port. we can emphasize that the techniques and tools that are used in angle measurement can be still improved through new methods and new hardware and software implementation.

Eventually, these research fields, for example, overhead crane, remote sensing, and so on, are a serial of hot spot studies, not only in the scientific research institution of the school but also in some crane companies in society.

References

- [1] "A Brief History of The Overhead Crane", Petercassidy.co.uk, 2014. [Online]. Available: <http://www.petercassidy.co.uk/a-brief-history-of-the-overhead-crane/>. [Accessed: 05- Sept- 2014].
- [2] "First Overhead Crane Company, Ludwig Stuckenholz is established ", Granada-cranes.co.uk, 2015. [Online]. Available: <https://www.granada-cranes.co.uk/1830-first-crane-company-established/>. [Accessed: 06- Aug- 2015].
- [3] "Sampson Moore supply the first overhead crane system in England", Granada-cranes.co.uk, 2015. [Online]. Available: <https://www.granada-cranes.co.uk/1876-first-electric-overhead-crane-system-in-england/>. [Accessed: 06- Aug- 2015].
- [4] "Electrical control systems introduced by Ludwig Stuckenholz", Granada-cranes.co.uk, 2015. [Online]. Available: <https://www.granada-cranes.co.uk/1887-ludwig-stuckenholz-introduces-electrical-control/>. [Accessed: 06- Aug- 2015].
- [5] "Leo Gottwald KG Builds the first mobile harbour crane", Granada-cranes.co.uk, 2015. [Online]. Available: <https://www.granada-cranes.co.uk/1918-leo-gottwald-kg-builds-the-first-mobile-harbour-crane/>. [Accessed: 06- Aug- 2015].
- [6] "Types of Overhead Cranes, Bridge Cranes", Aceindustries.com, 2020. [Online]. Available: <https://www.aceindustries.com/c-197-types-of-overhead-cranes-bridge-cranes.aspx>. [Accessed: 06- Oct- 2020].
- [7] "Gantry Cranes", Spanco.com, 2020. [Online]. Available: <https://www.spanco.com/products/gantry-cranes/>. [Accessed: 06- Oct- 2020].
- [8] " Shipbuilding Sector ", Europa.eu, 2020. [Online]. Available: https://ec.europa.eu/growth/sectors/maritime/shipbuilding_en. [Accessed: 06- Oct- 2020].
- [9] " Crane Transport and Crane Beam Delivery ", Cranesdq.com, 2016. [Online]. Available: <https://www.cranesdq.com/crane-transport.html>. [Accessed: 05- May- 2016].
- [10] " Port Gantry Cranes: A General Overview ", Marineinsight.com, 2016. [Online]. Available: <https://www.marineinsight.com/ports/port-gantry-cranes-a-general-overview/>. [Accessed: 01- Jan- 2016].
- [11] S.Garrido, M. Abderrahim, A. Gimenez, R. Diez, C. Balaguer, "Anti-Swinging Input Shaping Control of an Automatic Construction Crane," 2008 IEEE Transactions on Automation Science and Engineering, vol. 5, no. 3, pp. 549- 557, July 2008.
- [12] M.B. Tarbia, J.M. Renno, and K.A.F. Moustafa, "Generalized design of an anti-swing fuzzy logic controller for an overhead crane with hoist," Journal of Vibration and Control, vol. 14, no. 3, pp. 319-346, 2008.
- [13] S.Ohtomo, and T.Murakami, "Estimation method for sway angle of payload with reaction force observer," published in: IEEE 13th Advanced Motion Control (AMC), Yokohama, Japan, Mar, 2014.
- [14] H. Sano, K.Sato, K.Ohishi, T.Miyazaki."Robust Design of Vibration Suppression Control System for Crane Using Sway Angle Observer Considering Friction

- Disturbance" IEEJ Transactions on Industry Applications Vol. 132 No. 3 pp. 357-365, 2012.
- [15] T. Murakami, N. Mizukami, S Sakaino, T, Tsuji, "Bilateral control using functional electrical stimulation with reaction torque observer," published in: IEEE 14th Advanced Motion Control (AMC), Auckland New Zealand Apr 2016.
- [16] Y.S. Kim, K.S. Hong, and S.K. Sul, "Anti-sway control of container cranes: Inclinometer, observer, and state feedback," Int. Journal of Control Automation and Systems, vol. 2, no. 4, pp. 435-449, Dec 2004.
- [17] A. Giua, M. Sanna, and C. Seatzu, "Observer controller design for three dimensional overhead cranes using time-scaling," Mathematical and Computer Modeling of Dynamical Systems, vol. 7, no. 1, pp. 77-107, 2001.
- [18] H. Osumi, A. Miura and S. Eiraku, "Positioning of wire suspension system using CCD cameras," Proc. Of IEEE/RSJ Int. Conf. Intell. Robots and Systems, pp.258-263, Aug 2005
- [19] L.Lee, P.Huang, Y.Shih, S.Ku and C.Chang, "Adaptive Fuzzy Sliding Mode Control to Overhead Crane by CCD Sensor," 2011 IEEE International Conference on Control Applications (CCA), pp, 474-478, Sept 2011.
- [20] General Electric Company, "Electronic Anti-sway Control," US patent number 5443566, 1992
- [21] " LIDAR Lite v3 Operation Manual and Technical Specifications ", static.garmin.com, 2020. [Online]. Available: http://static.garmin.com/pumac/LIDAR_Lite_v3_Operation_Manual_and_Technical_Specifications.pdf. [Accessed: 13- Oct- 2020].
- [22] " ISPI_LIDAR", static.garmin.com, 2020. [Online]. Available: https://static.garmin.com/pumac/ISPI_LIDAR.pdf. [Accessed: 13- Oct- 2020].
- [23] " Inter-intergrated circuit ", egr.msu.edu, 2020. [Online]. Available: https://www.egr.msu.edu/classes/ece480/capstone/fall09/group03/AN_hemmanur.pdf. [Accessed: 13- Oct- 2020].
- [24] " UM10204 I2C-bus specification and user manual ", nxp.com, 2020. [Online]. Available: <https://www.nxp.com/docs/en/user-guide/UM10204.pdf>. [Accessed: 13- Oct- 2020].
- [25] " I2C Info – I2C Bus, Interface and Protocol ", i2c.info, 2020. [Online]. Available: <https://i2c.info/i2c-bus-specification> . [Accessed: 13- Oct- 2020].
- [26] " LIDAR-Lite v3 ", thingbits.in, 2020. [Online]. Available: <https://www.thingbits.in/products/lidar-lite-v3> . [Accessed: 13- Oct- 2020].
- [27] " GARMIN SUPPORT CENTER LIDAR-LITE V3 ", support.garmin.com, 2020. [Online]. Available: <https://support.garmin.com/en-US/?partNumber=010-01722-00&tab=topics> . [Accessed: 13- Oct- 2020].
- [28] "Motion Sp25 Radar Sensor ", nanoradar.cn, 2020. [Online]. Available: <http://en.nanoradar.cn/Article/detail/id/377.html> . [Accessed: 13- Oct- 2020].

- [29] " White paper on SP25 millimeter wave radar ", nanoradar.cn, 2020. [Online]. Available: <http://en.nanoradar.cn/File/view/id/431.html> . [Accessed: 13- Oct- 2020].
- [30] " SP25 millimeter wave radar user manual ", nanoradar.cn, 2020. [Online]. Available: <http://en.nanoradar.cn/File/download/id/432.html> . [Accessed: 13- Oct- 2020].
- [31] "SP25 Radar Sensor para Detecção De Movimento & Collision Avoidance ", nanoradar.cn, 2020. [Online]. Available: <https://portuguese.alibaba.com/product-detail/sp25-radar-sensor-for-motion-detection-collision-avoidance-62457545133.html> . [Accessed: 13- Oct- 2020].
- [32] "Sp25 milímetros sensor de radar de onda uav evitar obstáculos radar uav altura fixa radar ", aliexpress.com, 2020. [Online]. Available: <https://pt.aliexpress.com/item/10000163136620.html> . [Accessed: 13- Oct- 2020].
- [33] " Introduction to Arduino Uno ", theengineeringprojects.com, 2020. [Online]. Available: <https://www.theengineeringprojects.com/2018/06/introduction-to-arduino-uno.html> . [Accessed: 13- Oct- 2020].
- [34] "ARDUINO UNO REV3 ", store.arduino.cc, 2020. [Online]. Available: <https://store.arduino.cc/arduino-uno-rev3>. [Accessed: 13- Oct- 2020].
- [35] "Overhead crane trolley ", gruasyaparejos.com, 2020. [Online]. Available: <https://www.gruasyaparejos.com/en/tag/overhead-crane-trolley/>. [Accessed: 13- Oct- 2020].
- [36] " Definition: What is a Jib Crane? ", raymondhandling.com, 2020. [Online]. Available: <https://raymondhandling.com/dictionary/jib-crane/>. [Accessed: 13- Oct- 2020].
- [37] "Multi-sensor Fusion in Automated Driving: A Survey", researchgate.net, 2020. [Online]. Available: <https://link.springer.com/article/10.1631/FITEE.1900518>. [Accessed: 19- Oct- 2020].
- [38] "Multi-sensor Fusion in Automated Driving: A Survey", researchgate.net, 2020. [Online]. Available: https://www.researchgate.net/publication/338181839_Multi-sensor_Fusion_in_Automated_Driving_A_Survey. [Accessed: 19- Oct- 2020].
- [39] "RADAR- Basics, Types & Applications", *elprocus.com*, 2020. [Online]. Available: <https://www.elprocus.com/radar-basics-types-and-applications/>. [Accessed: 19- Oct- 2020].
- [40] " RADAR – Types & Its Application ", eeweb.com, 2020. [Online]. Available: <https://www.eeweb.com/radar-types-its-application/> . [Accessed: 19- Oct- 2020].
- [41] "No one knows wide area high frequency surveillance like we do", baesystems.com, 2020. [Online]. Available: <https://www.baesystems.com/en/feature/seeing-over-the-horizon>. [Accessed: 19- Oct- 2020].
- [42] "JORN: Australian Defence Force (ADF) OTH radar", blogspot.com, 2015. [Online]. Available: <http://i56578-sw1.blogspot.com/2015/02/jorn-australian-defence-force-adf-oth-b.html> . [Accessed: 19- Oct- 2020].

- [43] "Air Traffic Control Radar", radartutorial.eu, 2020. [Online]. Available: <https://www.radartutorial.eu/02.basics/ATC-Radars.en.html>. [Accessed: 19- Oct- 2020].
- [44] "Ground Traffic Control", abodynamics.com, 2020. [Online]. Available: <https://www.abodynamics.com/en/products/track-testing/ground-traffic-control> . [Accessed: 19- Oct- 2020].
- [45] "Radar remote sensing", bgr.bund.de, 2020. [Online]. Available: https://www.bgr.bund.de/EN/Themen/GG_Fernerkundung/Radarfernerkundung/radarfernerkundung_node_en.html. [Accessed: 19- Oct- 2020].
- [46] "Weather Radar Observations", community.wmo.int, 2020. [Online]. Available: <https://community.wmo.int/activity-areas/weather-radar-observations>. [Accessed: 19- Oct- 2020].
- [47] "What is LiDAR technology and how does it work?", geospatialworld.net, 2020. [Online]. Available: <https://www.geospatialworld.net/blogs/what-is-lidar-technology-and-how-does-it-work/>. [Accessed: 19- Nov- 2020].
- [48] "Leica TerrainMapper-2", geo-matching.com, 2020. [Online]. Available: <https://geo-matching.com/airborne-laser-scanning/leica-terrainmapper-2-increasing-your-productivity-for-complex-regional-regional-lidar-projects> . [Accessed: 19- Nov- 2020].
- [49] "Geomorphological Mapping", sciencedirect.com, 2011. [Online]. Available: <https://www.sciencedirect.com/topics/earth-and-planetary-sciences/terrestrial-laser-scanning>. [Accessed: 19- Nov- 2020].
- [50] "For the highest data density needs, lasers are the solution", sam.biz, 2020. [Online]. Available: <https://www.sam.biz/about/technology/terrestrial-lidar> . [Accessed: 19- Nov- 2020].
- [51] " Simscape Model and simulate multidomain physical systems", mathworks.com, 2020. [Online]. Available: <https://www.mathworks.com/products/simscape.html> . [Accessed: 30- Nov- 2020].
- [52] " Simscape Multibody Model and simulate multibody mechanical systems", mathworks.com, 2020. [Online]. Available: https://www.mathworks.com/products/simmechanics.html?s_tid=srchtitle . [Accessed: 30- Nov- 2020].
- [53] " Math. Graphics. Programming.", mathworks.com, 2020. [Online]. Available: <https://www.mathworks.com/products/matlab.html> . [Accessed: 30- Nov- 2020].

Annex A

Designações em português e inglês a colocar na capa da Dissertação

Português	Inglês
Departamento de Ciências e Tecnologias da Informação	Department of Information Science and Technology
Dissertação submetida como requisito parcial para obtenção do grau de	Dissertation submitted as partial fulfillment of the requirements for the degree of
Mestrado em Engenharia de Telecomunicações e Informática	Master in Telecommunications and Computer Engineering
Mestrado em Engenharia Informática	Master in Computer Engineering
Mestrado em Gestão de Sistemas de Informação	Master in Information Systems Management
Mestrado em Informática e Gestão	Master in Computer Science and Business Management
Mestrado em Sistemas Integrados de Apoio à Decisão	Master in Business Intelligence
Mestrado em Software de Código Aberto	Master in Open Source Software

Annex B

B-1 Multibody model anatomy

1) Basic Model Components: At its core, a multibody system is a set of bodies linked through joints and bound by kinematic constraints such as gears. Forces and torques of various types enable you to actuate the various bodies, while sensors enable you to sense the resulting motion. Other common blocks in a model include World Frame, Rigid Transform, Mechanism configuration, and Solver configuration.

2) Model Actuation can actuate a model by applying a force or torque to a body or to a joint. To represent forces and torques acting on a body, Simscape Multibody provides a Forces and Torques library. There are some types of force or torque, which include External Force and Torque, Internal Force, Spring and Damper Force, Inverse Square Law Force, and Gravitational Field. Joint actuation inputs can be of two types: Motion and Force or torque.

3) Dynamical Sensing can sense various dynamical variables between frame pairs, e.g., for analysis or control design. Sensing outputs can be of two types: Motion and Force or torque. Joint blocks enable you to sense different types of forces and torques between their respective port frames, including Actuation force or torque, Constraint force and torque, and Total force and torque.

As shown in Figure B1.1, it is Transform Sensor, which measures the spatial relationship between two frames. It also provides the broadest motion sensing capability. This is an extremely important block in Dynamical Sensing.



Figure B1.1 – Transform sensor

Creating a multibody model

Some steps for creating a Multibody Model:

Step 1: Study the System to Model

Identify the relevant bodies, joints, and constraints to incorporate in your model. Obtain the dimensions, inertia, and color of each solid as shown in Figure B1.2.

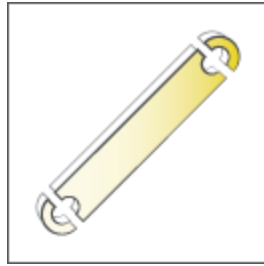


Figure B1.2 – Transform sensor

Step 2: Model the Bodies

Specify the solid properties of the various bodies. Add frames to the bodies so that you can connect joints and constraints, apply forces and torques, and sense motion as shown in Figure B1.3.

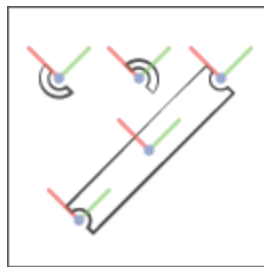


Figure B1.3 – Adding frames to each body

Step 3: Assemble the Multibody System

Connect the bodies by pairs through joints, gears, and constraints. Constrain body motion through gears and other kinematic constraints. Create and connect the frames required to assemble the various body elements into a complete body as shown in Figure B1.4.

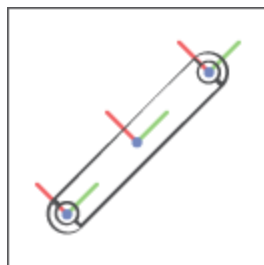


Figure B1.4 – Integrate several components

Step 4: Specify and Sense Dynamic Variables

There are model external loads, interactions between bodies, and joint actuation inputs. Sense forces, torques, and motion variables as functions of time. Visualize each body and verify its geometry, color, and frames in Figure B1.5.

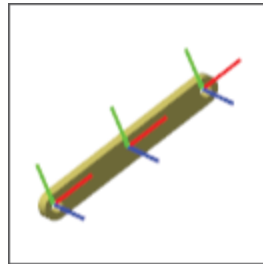


Figure B1.5 – Visualize each body check its profile

B-2 A multibody model example

When we click the Simscape in Figure 40, the Simscape will expand the options, which include Generic Simscape (1), Electrical, Electrical Three-Phase, Gas, and others. There are 14 physical functional models in total. Among these models, the Multibody model (2) is one special option for this project.

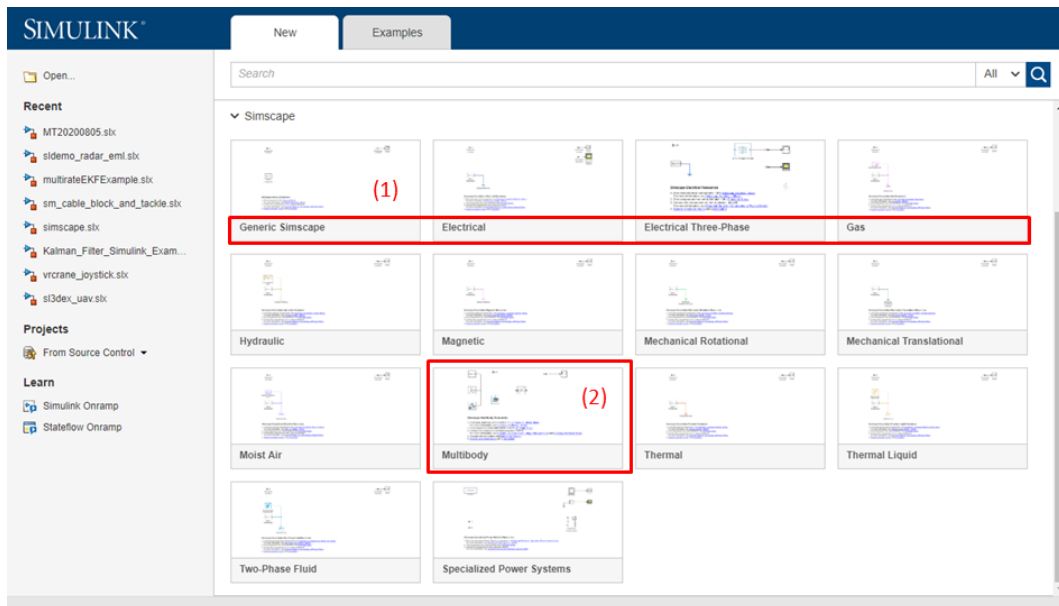


Figure B2.1 – All of Simscape products

Test in a single simulation environment to identify integration issues. The basic multibody example can be started. The basic components shown in Figure 41, which consist of Solver configuration (1), World Frame blocks (2), Mechanism Configuration (3), Rigid Transform (4), Brick Solid (5), and Scope (6).

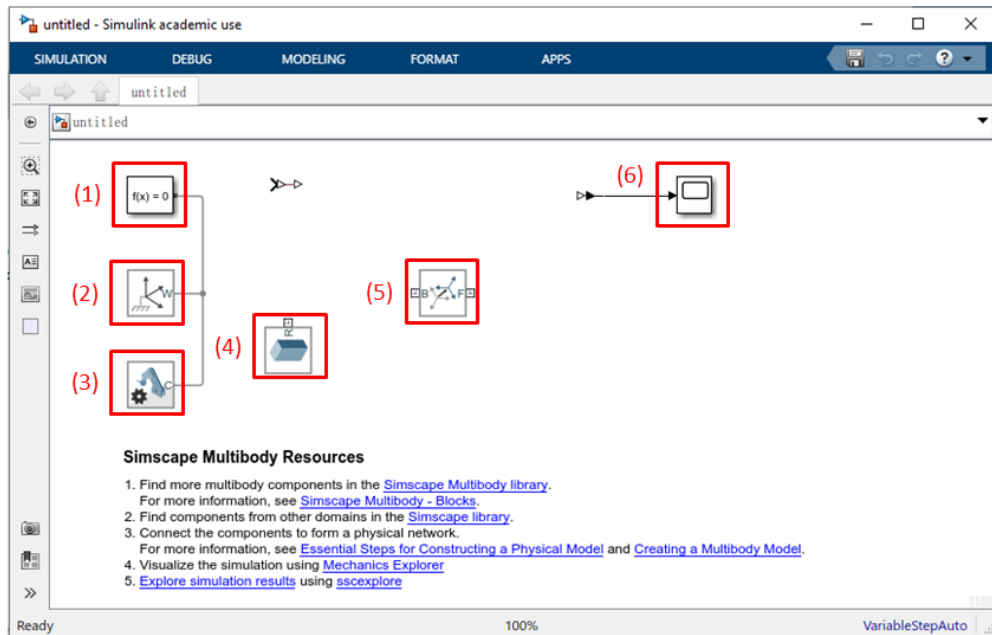


Figure B2.2 – An example for the multibody

- Solver configuration -- Defines solver settings to use for simulation.
- World Frame blocks -- Provides access to the world or ground frame, a unique motionless, orthogonal, right-handed coordinate frame predefined in any mechanical model. World frame is the ground of all frame networks in a mechanical model.
- Mechanism Configuration -- Sets mechanical and simulation parameters that apply to an entire machine, the target machine to which the block is connected. In the Properties section below, you can specify uniform gravity for the entire mechanism and also set the linearization delta.
- Rigid Transform -- Defines a fixed 3-D rigid transformation between two frames. Two components independently specify the translational and rotational parts of the transformation. Different translations and rotations can be freely combined.
- Brick Solid -- Represents a solid combining a geometry, an inertia and mass, a graphics component, and rigidly attached frames into a single unit.
- Scope -- Displays time domain signals.

B-3 SP25 Specifications

Pins	Definition	Range
1	Power In	4-6V DC
2	\	\
3	GND	\
4	\	\
5	TTL USART_RX	0~3.3V DC
6	TTL USART_TX	0~3.3V DC
7	\	\
8	\	\
9	\	\
10	\	\

B-4 Arduino Uno Rev3 specifications

Item	Definition
Microcontroller	ATmega328P
Operating Voltage	5V
Input Voltage (recommended)	7-12V
Input Voltage (limit)	6-20V
Digital I/O Pins	14 (of which 6 provide PWM output)
PWM Digital I/O Pins	6
Analog Input Pins	6
DC Current per I/O Pin	20 mA
DC Current for 3.3V Pin	50 mA
Flash Memory	32 KB (ATmega328P) of which 0.5 KB used by bootloader


SRAM	2 KB (ATmega328P)
EEPROM	1 KB (ATmega328P)
Clock Speed	16 MHz
LED_BUILTIN	13
Length	68.6 mm
Width	53.4 mm

Annex C

One of my paper have been uploaded to 2021 Telecoms Conference (ConfTELE).

The website of conference is that: <http://conftele2021.ipleiria.pt/index.html>

The title of paper is that “Microwave Radar Based Estimation of the Sway Angle of Payload in Overhead Crane System”, as shown in Figure C.1.



The screenshot shows the ConfTELE 2021 website interface. At the top, there is a banner for "CONFTELE 2021 TELECOMS CONFERENCE" held from "11-12 FEB" in "LISBOA, PORTUGAL". Below the banner is a navigation menu with "Home", "Register", "Travel grants", "My...", and "Help". The main content area displays the paper title: "#32 (1570692545): Microwave Radar Based Estimation of the Sway Angle of Payload in Overhead Crane System". A "bib" icon is visible below the title. Below the title is a table with columns for "Property", "Change Add", and "Value". The table lists the conference as "2021 Telecoms Conference (ConfTELE) - Main Track" and the authors as Yibin Hu, Octavian Adrian Postolache, and another author (partially obscured).

Property	Change Add	Value																											
Conference and track		2021 Telecoms Conference (ConfTELE) - Main Track																											
Authors		<table border="1"> <thead> <tr> <th>Name</th> <th>ID</th> <th>Edit</th> <th>Flag</th> <th>Affiliation (edit for paper)</th> <th>Email</th> <th>Country</th> <th>Email</th> <th>Delete</th> </tr> </thead> <tbody> <tr> <td>Yibin Hu</td> <td>1819357</td> <td></td> <td></td> <td>ISCTE - Instituto Universitário de Lisboa, Portugal</td> <td>albertybhu@gmail.com</td> <td>Portugal</td> <td></td> <td></td> </tr> <tr> <td>Octavian Adrian Postolache</td> <td>105638</td> <td></td> <td></td> <td>Instituto de Telecomunicações, Lisboa/IT & Instituto Universitario de Lisboa, ISCTE-IUL, Portugal</td> <td>octavian.postolache@gmail.com</td> <td>Portugal</td> <td></td> <td></td> </tr> </tbody> </table>	Name	ID	Edit	Flag	Affiliation (edit for paper)	Email	Country	Email	Delete	Yibin Hu	1819357			ISCTE - Instituto Universitário de Lisboa, Portugal	albertybhu@gmail.com	Portugal			Octavian Adrian Postolache	105638			Instituto de Telecomunicações, Lisboa/IT & Instituto Universitario de Lisboa, ISCTE-IUL, Portugal	octavian.postolache@gmail.com	Portugal		
Name	ID	Edit	Flag	Affiliation (edit for paper)	Email	Country	Email	Delete																					
Yibin Hu	1819357			ISCTE - Instituto Universitário de Lisboa, Portugal	albertybhu@gmail.com	Portugal																							
Octavian Adrian Postolache	105638			Instituto de Telecomunicações, Lisboa/IT & Instituto Universitario de Lisboa, ISCTE-IUL, Portugal	octavian.postolache@gmail.com	Portugal																							

Figure C.1 – The uploaded paper in the 2021 Telecoms Conference